Safety and Efficacy of Allogeneic Cell Therapy in Infarcted Rats Transplanted With Mismatched Cardiosphere-Derived Cells

Konstantinos Malliaras, Tao-Sheng Li, Daniel Luthringer, John Terrovitis, Ke Cheng, Tarun Chakravarty, Giselle Galang, Yiqiang Zhang, Florian Schoenhoff, Jennifer Van Eyk, Linda Marbán and Eduardo Marbán

Circulation. 2012;125:100-112; originally published online November 15, 2011;
doi: 10.1161/CIRCULATIONAHA.111.042598
Circulation is published by the American Heart Association, 7272 Greenville Avenue, Dallas, TX 75231

Print ISSN: 0009-7322. Online ISSN: 1524-4539

Safety and Efficacy of Allogeneic Cell Therapy in Infarcted Rats Transplanted With Mismatched Cardiosphere-Derived Cells

Konstantinos Malliaras, MD; Tao-Sheng Li, MD, PhD; Daniel Luthringer, MD; John Terrovitis, MD; Ke Cheng, PhD; Tarun Chakravarty, MD; Giselle Galang, BS; Yiqiang Zhang, PhD; Florian Schoenhoff, MD; Jennifer Van Eyk, PhD; Linda Marbán, PhD; Eduardo Marbán, MD, PhD

Background—Cardiosphere-derived cells (CDCs) are an attractive cell type for tissue regeneration, and autologous CDCs are being tested clinically. However, autologous therapy necessitates patient-specific tissue harvesting and cell processing, with delays to therapy and possible variations in cell potency. The use of allogeneic CDCs, if safe and effective, would obviate such limitations. We compared syngeneic and allogeneic CDC transplantation in rats from immunologically-mismatched inbred strains.

Methods and Results—In vitro, CDCs expressed major histocompatibility complex class I but not class II antigens or B7 costimulatory molecules. In mixed-lymphocyte cocultures, allogeneic CDCs elicited negligible lymphocyte proliferation and inflammatory cytokine secretion. In vivo, syngeneic and allogeneic CDCs survived at similar levels in the infarcted rat heart 1 week after delivery, but few syngeneic (and even fewer allogeneic) CDCs remained at 3 weeks. Allogeneic CDCs induced a transient, mild, local immune reaction in the heart, without histologically evident rejection or systemic immunogenicity. Improvements in cardiac structure and function, sustained for 6 months, were comparable with syngeneic and allogeneic CDCs. Allogeneic CDCs stimulated endogenous regenerative mechanisms (cardiomyocyte cycling, recruitment of c-kit$^+$ cells, angiogenesis) and increased myocardial vascular endothelial growth factor, insulin-like growth factor-1, and hepatocyte growth factor equally with syngeneic CDCs.

Conclusions—Allogeneic CDC transplantation without immunosuppression is safe, promotes cardiac regeneration, and improves heart function in a rat myocardial infarction model, mainly through stimulation of endogenous repair mechanisms. The indirect mechanism of action rationalizes the persistence of benefit despite the evanescence of transplanted cell survival. This work motivates the testing of allogeneic human CDCs as a potential off-the-shelf product for cellular cardiomyoplasty. **(*Circulation*. 2012;125:100-112.)**

Key Words: allogeneic transplantation ■ paracrine communication ■ regeneration ■ stem cells

Cell transplantation has emerged as a promising therapeutic strategy for acute or chronic ischemic cardiomyopathy.[1,2] Multiple candidate cell types have been used in humans in efforts to repair or regenerate the injured heart either directly (through formation of new transplanted tissue) or indirectly, including skeletal myoblasts, bone marrow–derived cells, and, more recently, heart-derived cells.[2,3] During the first decade of cell therapy for heart disease, the vast majority of clinical trials were conducted with autologous cells. This approach avoids immunologic rejection but necessitates patient-specific tissue harvesting, cell processing, and quality control, imposing significant logistic, economic, and timing constraints. In addition, cell efficacy may be undermined by donor age and comorbidities.[4] The use of allogeneic cells, if safe and effective, would obviate such limitations, enabling the generation of highly standardized off-the-shelf cell products. The obvious disadvantage is the risk of immune rejection, which may limit effectiveness regardless of whether it poses safety hazards. Nevertheless, because the vast majority of the observed functional benefit is attributable to indirect pathways even with heart-derived cells,[5,6] rejection of allogeneic cells may not be an issue if it occurs after the cells have exerted their beneficial paracrine effects and if the resulting benefits are durable.

Clinical Perspective on p 112

Here, we tested the hypothesis that allogeneic cardiosphere-derived cells (CDCs) are hypoimmunogenic

Received May 8, 2011; accepted October 27, 2011.

From the Cedars-Sinai Heart Institute, Los Angeles, CA (K.M., T.-S.L., D.L., J.T., K.C., T.C., G.G., Y.Z., L.M., E.M.), and Department of Medicine, Division of Cardiology, Johns Hopkins Bayview Proteomics Center, Johns Hopkins University, Baltimore, MD (F.S., J.V.E.).

The online-only Data Supplement is available with this article at http://circ.ahajournals.org/lookup/suppl/doi:10.1161/CIRCULATIONAHA.111.042598/-/DC1.

Correspondence to Eduardo Marbán, MD, PhD, Cedars-Sinai Heart Institute, 8700 Beverly Blvd, Los Angeles, CA 90048. E-mail Eduardo.Marban@csmc.edu

and mobilize pathways of endogenous repair and regeneration, resulting in sustained functional benefit. For the first time, we characterize the in vitro immunologic properties of heart-derived stem cells, monitor host immune system kinetics (leukocyte infiltration, inflammatory cytokine secretion, development of cellular/humoral memory response) and transplanted cell survival, and quantify functional effects after myocardial infarction (MI) in an immunologically-mismatched rat model of allogeneic CDC transplantation.

Methods

An expanded Methods section is available in the online-only Data Supplement.

Experimental Animals

To create a stringent model of allogeneic cell transplantation, we used rats from highly-inbred, immunologically-divergent strains characterized by complete mismatch of major histocompatibility complex (MHC) antigens. Male Wistar-Kyoto (WKY) rats (MHC haplotype, RTI^l) were used as CDC donors; female WKY and Brown Norway (BN) rats (MHC haplotype, RTI^n) were used as syngeneic and allogeneic recipients, respectively. In a model of xenogeneic transplantation used as a positive control for immune rejection, human CDCs (hCDCs) were transplanted into BN rats. Sample sizes for each experiment are listed in Table I in the online-only Data Supplement. All experimental protocols were approved by the Institutional Animal Care and Use Committee.

Cell Culture

Rat CDCs (rCDCs) were expanded from 8-week old male WKY rat hearts. hCDCs were expanded from endomyocardial biopsies or myocardial samples obtained from adult male patients during clinically indicated procedures after informed consent was given. Patient characteristics are presented in Table II in the online-only Data Supplement. CDCs were cultured as described.[7,8] All experiments were performed with CDCs at passage 1. In a subset of experiments, CDCs were lentivirally transduced to express green fluorescent protein (GFP) to track transplanted cell fate by histology.

Flow Cytometry

Flow cytometry was performed to evaluate surface expression of MHC class I, MHC class II, and costimulatory molecules (CD80, CD86) in hCDCs and rCDCs under baseline conditions and after stimulation with interferon-γ (IFN-γ). In addition, we characterized the general phenotype of CDCs (expression of CD105, c-Kit, CD90, CD31, CD45, CD140b, discoidin domain-containing receptor 2, and α-smooth muscle actin; antibodies listed in Table III in the online-only Data Supplement).

Mixed-Lymphocyte Reactions

The in vitro immunogenicity of CDCs was assessed by 1-way mixed-lymphocyte reactions. Mitomycin-inactivated stimulating rCDCs and hCDCs were cocultured with responder lymphocytes for 5 days. Responder cell proliferation was assessed by BrdU incorporation. The following experimental conditions were tested: rCDCs cocultured with WKY lymphocytes (syngeneic coculture), rCDCs cocultured with BN lymphocytes (allogeneic coculture), and hCDCs cocultured with BN lymphocytes (xenogeneic coculture). Alloreactive and xenoreactive lymphocyte proliferation is presented as relative proliferative response normalized to syngeneic lymphocyte proliferation (stimulation index). The cell-free supernatant of the cocultures was collected, and the levels of secreted IFN-γ, interleukin (IL)-1b, IL-13, IL-4, IL-5, KC/GRO (Chemokine [C-X-C motif] ligand 1), tumor necrosis factor-α, and IL-2 were measured by electrochemiluminescence and ELISA.

MI and Cell Injection

Female WKY and BN rats (8–10 week old) underwent permanent ligation of the left anterior descending coronary artery. CDCs (2 million suspended in 120 μL PBS) or vehicle were injected intramyocardially at 4 sites along the periphery of the infarct. Five permutations were investigated: rCDCs injected into WKY hearts (syngeneic group), rCDCs injected into BN hearts (allogeneic group), hCDCs injected into BN hearts (xenogeneic group), vehicle injected into WKY hearts (control group a), and vehicle injected into BN hearts (control group b). Two control groups were used to confirm that both rat strains responded similarly to MI. Data for perioperative and longer-term mortality are presented in Table IV in the online-only Data Supplement. To monitor proliferation of both transplanted and endogenous cells, a subset of animals were injected intraperitoneally with BrdU daily for either the first week or the second and third weeks after MI.

Echocardiography

Echocardiography was performed to assess global cardiac function 6 hours (baseline), 3 weeks, 3 months, and 6 months after surgery. Fractional area change, left ventricular ejection fraction, and fractional shortening were measured.

Quantification of Engraftment by Real-Time Polymerase Chain Reaction

To monitor transplanted cell survival 1 and 3 weeks after MI, male cells were injected into female rats, and absolute cell engraftment was quantified with the use of species-specific SRY gene primers.

Histology

Rats were euthanized 1 week, 3 weeks, and 6 months after treatment. Hearts were cryosectioned and fixed with 4% paraformaldehyde. Quantitative morphometric analysis with Masson trichrome staining was performed to quantify scar size, infarcted wall thickness, and left ventricular remodeling. To evaluate immune rejection, sections stained with hematoxylin and eosin were evaluated in a blinded manner by a cardiac pathologist (D.L); in addition, immunostaining against immune cell markers was performed. Differentiation of CDCs, incidence of cycling host myocytes, recruitment of endogenous progenitors, and vessel density in the border zone were evaluated by immunohistochemistry (antibodies listed in Table III in the online-only Data Supplement).

Assessment of Systemic Immunogenicity and Development of Memory Immune Response

To assess systemic immunogenicity, levels of circulating inflammatory cytokines (IFN-γ, IL-1b, IL-13, IL-4, IL-5, KC/GRO, and tumor necrosis factor-α) were quantified by electrochemiluminescence in rat sera from recipients of syngeneic, allogeneic, and xenogeneic CDCs and controls.

To assess humoral memory immune response, recipient rat sera were isolated 1 and 3 weeks after transplantation, and levels of circulating alloreactive and xenoreactive anti-donor IgG and IgM antibodies were quantified by flow cytometry.

To evaluate cellular memory immune response, spleens from allogeneic recipients were harvested 3 weeks after transplantation. Lymphocytes were isolated, and their reactivity against allogeneic donor cells by 1-way mixed-lymphocyte reactions was compared with that of naïve lymphocytes. The cell-free supernatant of the cocultures was collected, and the levels of secreted IFN-γ, IL-1b, IL-13, IL-4, IL-5, KC/GRO, tumor necrosis factor-α, and IL-2 were measured by electrochemiluminescence and ELISA.

Western Blotting

Western blot analysis was performed to compare myocardial levels of vascular endothelial growth factor, insulin-like growth factor-1, and hepatocyte growth factor at various time points after MI in rat hearts from the syngeneic, allogeneic, xenogeneic, and control groups. Myocardial samples from the peri-infarct area were collected

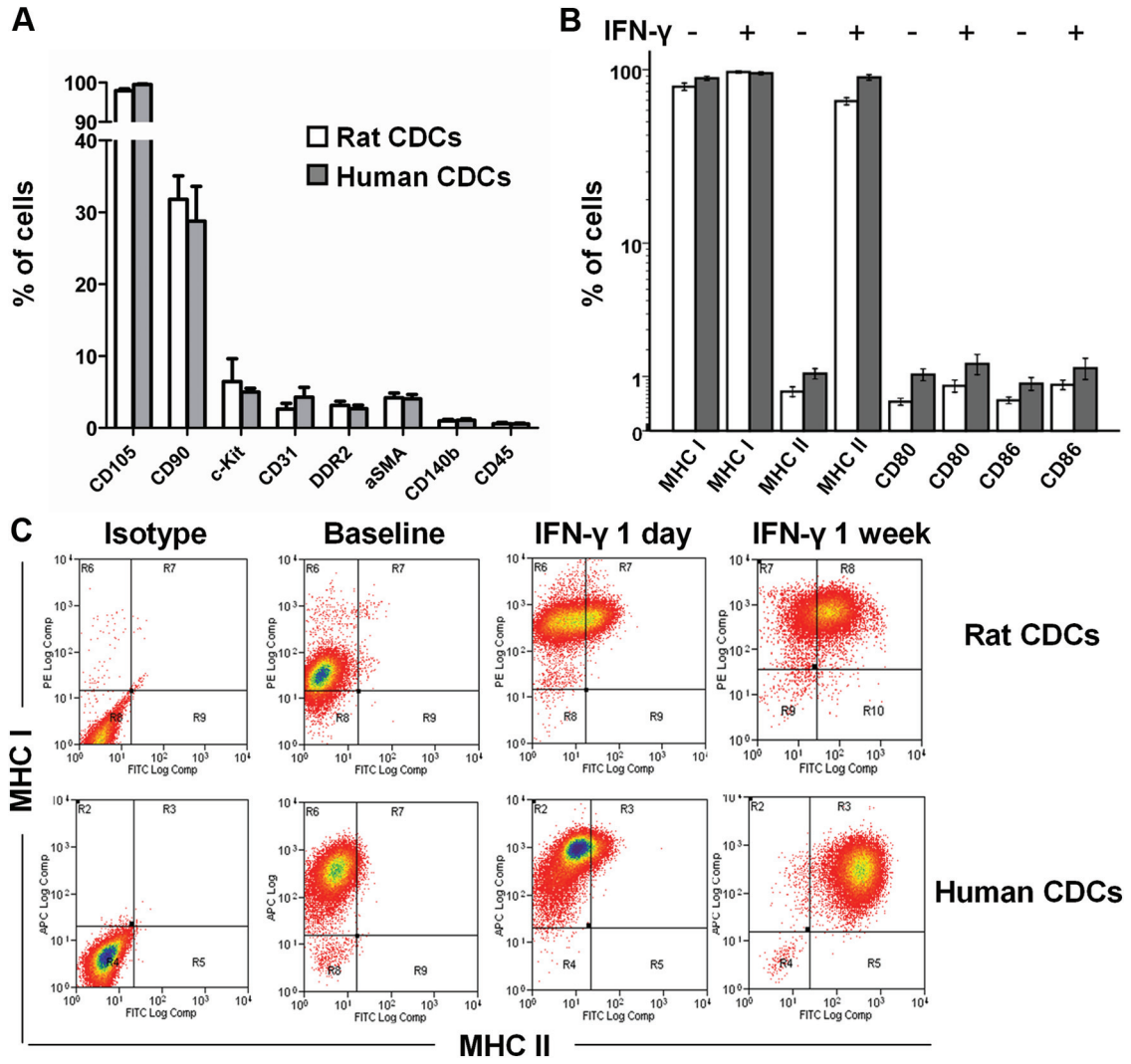

Figure 1. Phenotypic characterization of rat and human cardiosphere-derived cells (CDCs) by flow cytometry. **A**, Antigenic profiles of CDCs (n=4–5 per group). **B**, Immunophenotype of CDCs under baseline conditions and after interferon-γ (IFN-γ) stimulation (n=4–5/group). **C**, CDCs at baseline express major histocompatibility complex (MHC) class I but not MHC class II antigens. Incubation with IFN-γ upregulates expression of MHC class I and class II antigens in a time-dependent manner.

5 minutes, 1 day, 4 days, 7 days, and 21 days after MI. Protein was extracted and Western blots were performed as described[5] with the antibodies listed in Table III in the online-only Data Supplement.

Statistical Analysis

Results are presented as means±SEM. Normality of data was tested by use of the Shapiro-Wilk test, and equality of variances was tested with the Levene test. If normality of data and equality of variances were established, statistical significance was determined by 1-way ANOVA followed by the Bonferroni post hoc test. If normality of data or equality of variances could not be confirmed, statistical significance was determined by the Kruskal-Wallis test followed by the Dunn post hoc test. Linear mixed-effects models were used to compare the repeated measurements of cardiac function across groups. The outcome was the dependent variable; treatment group and time were the fixed effects; and an unstructured trend in time was assumed. Correlation in data from the same animal was taken into account by a random effect at the rat level. Categorical data were tested by the Fisher exact test. Differences between 2 groups were tested with the Mann-Whitney *U* test. Differences were considered significant when $P<0.05$.

Results

Characterization of CDC Antigens Including MHC and Costimulatory Molecules

Consistent with previous characterizations,[7,9] flow cytometry revealed that both rCDCs and hCDCs are naturally heterogeneous cell populations of nonhematological origin ($CD45^-$) that are positive for CD105; subgroups positive for c-kit or CD90 are consistent with cardiac progenitor and cardiac mesenchymal fractions, respectively, whereas <4% of cells are positive for fibroblast (discoidin domain-containing receptor 2) or myofibroblast (α-smooth muscle actin) markers (Figure 1A). With regard to immune antigens, both rCDCs and hCDCs express MHC class I but not MHC class II surface antigens or CD80/CD86 costimulatory molecules under baseline conditions (Figure 1B). Incubation with IFN-γ upregulated MHC class I and MHC class II expression (but not costimulatory molecule expression) in a time-dependent manner (Figure 1B and 1C). The observed baseline immuno-

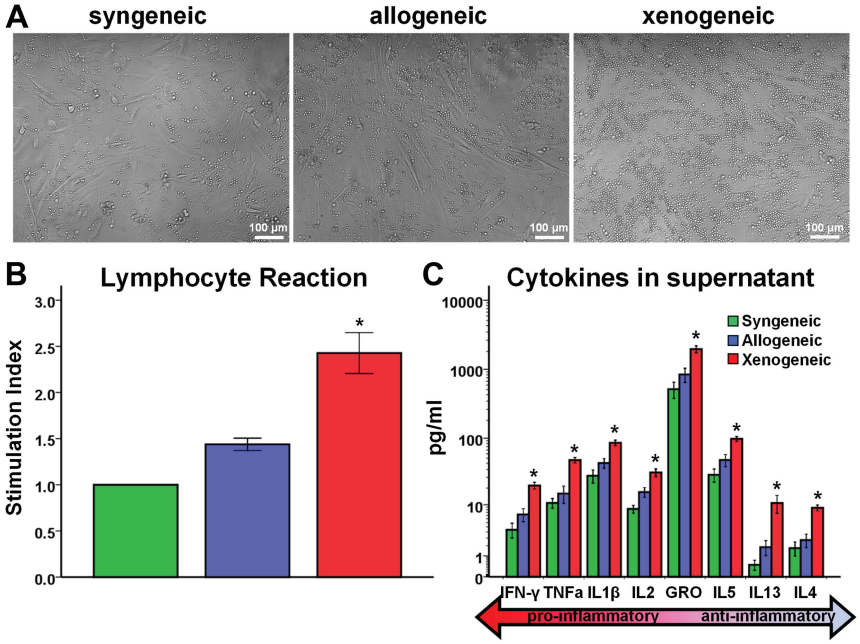

Figure 2. Assessment of immunogenicity of cardiosphere-derived cells (CDCs) in vitro. **A**, Representative images of syngeneic, allogeneic, and xenogeneic cocultures. Significant lymphocyte proliferation can be observed in the xenogeneic setting. Quantitative analyses of (**B**) responder cell proliferation (n=6–8 per group) and (**C**) inflammatory cytokine secretion (n=21–26 per group) demonstrate that allogeneic CDCs, contrary to xenogeneic cultures, exhibit negligible functional immunogenicity in vitro (*$P<0.05$ vs syngeneic and allogeneic groups). IFN-γ indicates interferon-γ; TNFa, tumor necrosis factor-α, and IL, interleukin.

phenotype of CDCs renders them attractive for allogeneic applications. Expression of MHC class I antigens is important because it protects cells from natural killer cell–mediated deletion,[10] whereas lack of expression of MHC class II antigens allows CDCs to escape direct recognition from $CD4^+$ T helper cells. MHC class I antigens may activate effector T cells, but in the absence of costimulatory molecules, a secondary signal would not engage, theoretically leaving T cells anergic.[11]

Allogeneic CDCs Exhibit Negligible In Vitro Immunogenicity

One-way mixed-lymphocyte reaction experiments revealed that allogeneic rCDCs elicit negligible lymphocyte proliferation, comparable to that seen with syngeneic CDCs. On the other hand, xenogeneic hCDCs induce a strong proliferative response (Figure 2A and 2B). Levels of proinflammatory (IFN-γ, tumor necrosis factor-α, IL-1b, IL-2, KC/GRO) and antiinflammatory (IL-5, IL-13, IL-4) cytokines were comparable in syngeneic and allogeneic coculture supernatants. Conversely, in the xenogeneic setting, secretion of all inflammatory cytokines was markedly increased, indicating significant activation of responder lymphocytes (Figure 2C).

Limited Survival of Allogeneic and Syngeneic CDCs After Transplantation

Two million male syngeneic, allogeneic, or xenogeneic CDCs were implanted into the ischemic myocardium of female rats immediately after left anterior descending artery ligation. Quantitative polymerase chain reaction with the male SRY gene as target revealed that engraftment of allogeneic and syngeneic CDCs is similar 1 week after MI (Figure 3C). Three weeks after MI, cell survival decreases markedly (to <1% of cells transplanted) in both groups, but the residual number of surviving cells is higher after syngeneic transplantation (Figure 3D). These results indicate that allogeneic CDCs are cleared more rapidly than syngeneic CDCs between days 8 and 21 after delivery. On the other hand, the vast majority of xenogeneic CDCs are rejected within 1 week of transplantation (Figure 3C), with no surviving cells detectable 3 weeks after MI (Figure 3D). The observed prompt rejection of xenogeneic CDCs in immunocompetent hosts echoes previous findings.[12]

Allogeneic and Syngeneic CDCs Exert Comparable and Sustained Beneficial Effects on Infarcted Heart Structure and Function

Morphometric analysis of explanted hearts 3 weeks after MI showed severe left ventricular chamber dilatation and infarct wall thinning in animals in the xenogeneic and control groups (Figure 4A). In contrast, the syngeneic and allogeneic groups exhibited smaller scar size, increased infarcted wall thickness, and attenuation of left ventricular remodeling (Figure 4A–4C). Scar size and infarcted wall thickness did not differ among animals treated with syngeneic or allogeneic CDCs, suggesting similar favorable treatment effects in these 2 groups.

To investigate whether allogeneic cell transplantation offers functional benefit, global cardiac function was assessed by echocardiography. At baseline, fractional area change, left ventricular ejection fraction, and fractional shortening did not differ among treatment groups, indicating similar degrees of initial injury. Over the first 3 weeks after MI, indexes of function did not improve in the xenogeneic and control groups, whereas fractional area change, left ventricular ejection fraction, and fractional shortening all rose significantly, and to similar degrees, in the syngeneic and allogeneic groups. Notably, the functional benefit observed at 3 weeks persisted at 6 months (Figure 4D–4G). Thus, despite lower engraftment at 3 weeks, allogeneic CDCs pack the same punch functionally and structurally as syngeneic CDCs.

Allogeneic CDCs Are Hypoimmunogenic In Vivo

To evaluate the spatiotemporal development of immune rejection in the scar, border zone, and remote myocardium,

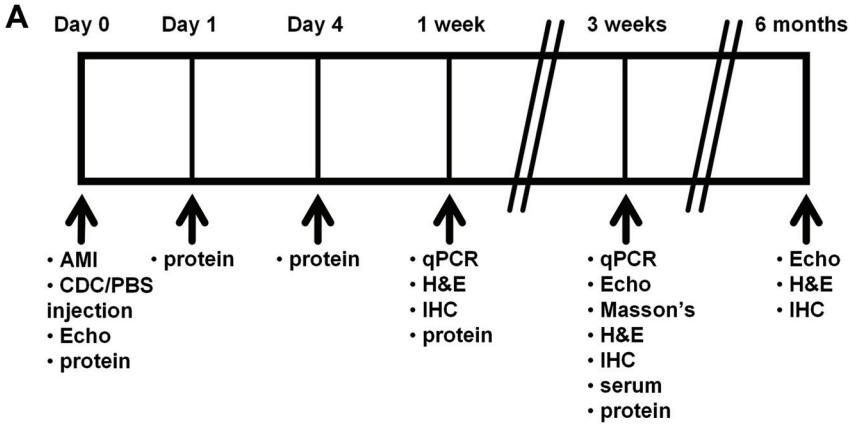

B

Group 1	Syngeneic model	n=40	WKY rats given 2*10^6 synCDCs after LAD ligation
Group 2	Allogeneic model	n=40	BN rats given 2*10^6 alloCDCs after LAD ligation
Group 3	Control group a	n=20	WKY rats given PBS after LAD ligation
Group 4	Control group b	n=20	BN rats given PBS after LAD ligation
Group 5	Xenogeneic model	n=40	BN rats given 2*10^6 human CDCs after LAD ligation

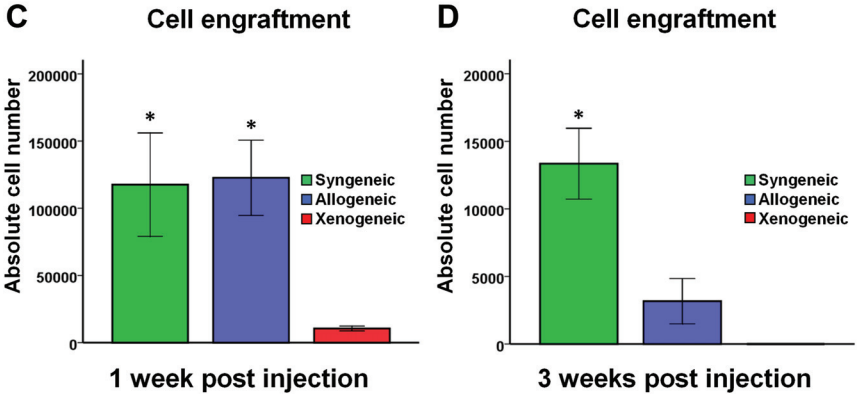

Figure 3. Study outline, experimental groups, and cardiosphere-derived cell (CDC) engraftment. **A**, Study outline. **B**, Experimental groups. **C**, Cell engraftment by quantitative polymerase chain reaction (qPCR) 1 week (n=5–6 per group) and (**D**) 3 weeks (n=5–6 per group) after myocardial infarction (MI) and cell transplantation. Syngeneic and allogeneic CDCs demonstrated similar survival rates 1 week after transplantation, whereas the vast majority of xenogeneic cells had already been rejected. Three weeks after transplantation, cell survival was poor in both the syngeneic and allogeneic groups but significantly higher after transplantation of syngeneic cells. No xenogeneic cells were detectable at 3 weeks (*$P<0.05$ vs xenogeneic group). AMI indicates acute MI; H&E, hematoxylin and eosin; IHC, immunohistochemistry; WKY, Wistar-Kyoto; BN, Brown Norway; and LAD, left anterior descending.

hematoxylin and eosin–stained sections obtained at 1 week, 3 weeks, and 6 months after treatment were evaluated with the International Society of Heart and Lung Transplantation grading system (used in clinical practice to diagnose rejection; Figure 5) and a homemade, more descriptive grading system (Tables V–VII in the online-only Data Supplement). No clear-cut immune rejection could be detected in the allogeneic setting at any time point. In contrast, xenogeneic cell transplantation resulted in grade 1R rejection, with significant mononuclear infiltration in the infarct scar and border zone 1 week (Figure 5B and 5C and Table V in the online-only Data Supplement) and 3 weeks (Figure 5D and 5E and Table VI in the online-only Data Supplement) after MI. The infiltrating cells were localized within interstitial and perivascular spaces (Figure 5A), but no foci of myocyte damage could be detected, even with xenogeneic CDCs. The remote myocardium was consistently clear of rejection, in agreement with previously observed homing of transplanted CDCs to the infarct and peri-infarct areas.[5,7]

Although clinically useful in the assessment of transplant rejection, detection of small foci of rejection by hematoxylin and eosin staining is complicated in a post-MI setting by the natural inflammatory response to the ischemic insult. Because our quantitative polymerase chain reaction data revealed disproportionate loss of allogeneic CDCs at 3 weeks, we performed extensive immunostaining to define the identity of the infiltrating inflammatory cells (Figure 6). In the allogeneic setting, immunohistochemistry revealed rare events of rejection; a few small and sparse infiltrates (some around transplanted cells [Figure 6A]) were detected 3 weeks after treatment in the infarct and peri-infarct areas, made up primarily of $CD3^+$ T lymphocytes (with equal contributions of $CD8^+$ T cytotoxic and $CD4^+$ T helper subpopulations) and, to a lesser extent, $CD45RA^+$ B lymphocytes and $CD11c^+$ dendritic cells. The similar amounts of $CD4^+$ and $CD8^+$ T lymphocytes and the presence of dendritic cells in the grafts hint at a more prominent role of the indirect pathway of allorecognition in the immune rejection of trans-

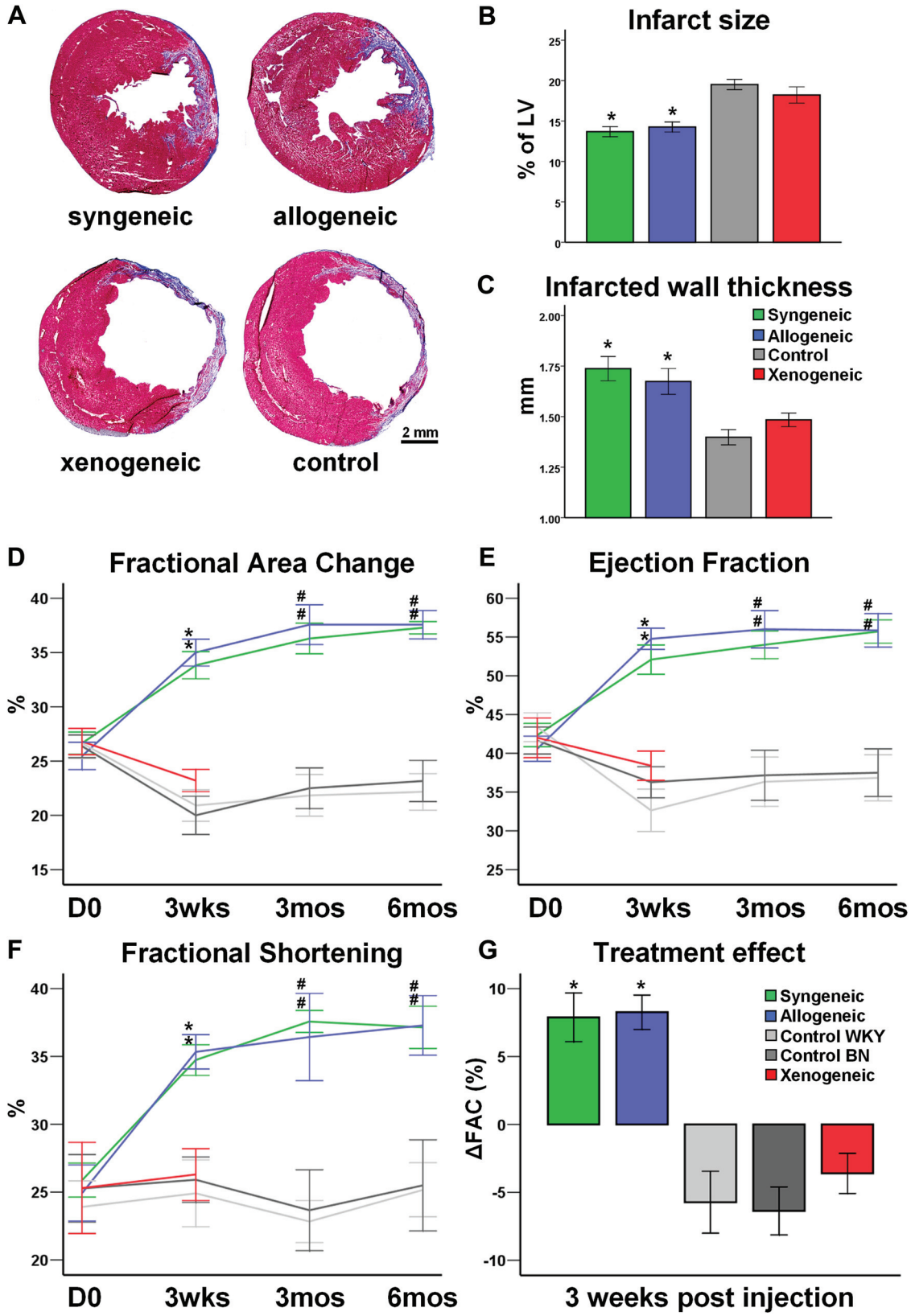

Figure 4. Structural and functional benefits after syngeneic and allogeneic cardiosphere-derived cell (CDC) transplantation. **A**, Representative images of Masson trichrome staining of infarcted rat hearts 3 weeks after myocardial infarction. Both syngeneic and allogeneic transplantation reduced infarct size (**B**) and increased infarcted wall thickness (**C**) compared with the xenogeneic or control group (n=5–8 per group). Echocardiographic assessment of left ventricular (LV) function revealed that both syngeneic and allogeneic CDC transplantation resulted in a robust and sustained improvement of fractional area change (FAC; **D**), ejection fraction (**E**), and fractional shortening (**F**). The treatment effect was similar in the syngeneic and allogeneic groups (**G**) and was sustained at least for 6 months (*$P<0.05$ vs xenogeneic and control groups; #$P<0.05$ vs control group; sample sizes for D–G listed in Table I in the online-only Data Supplement).

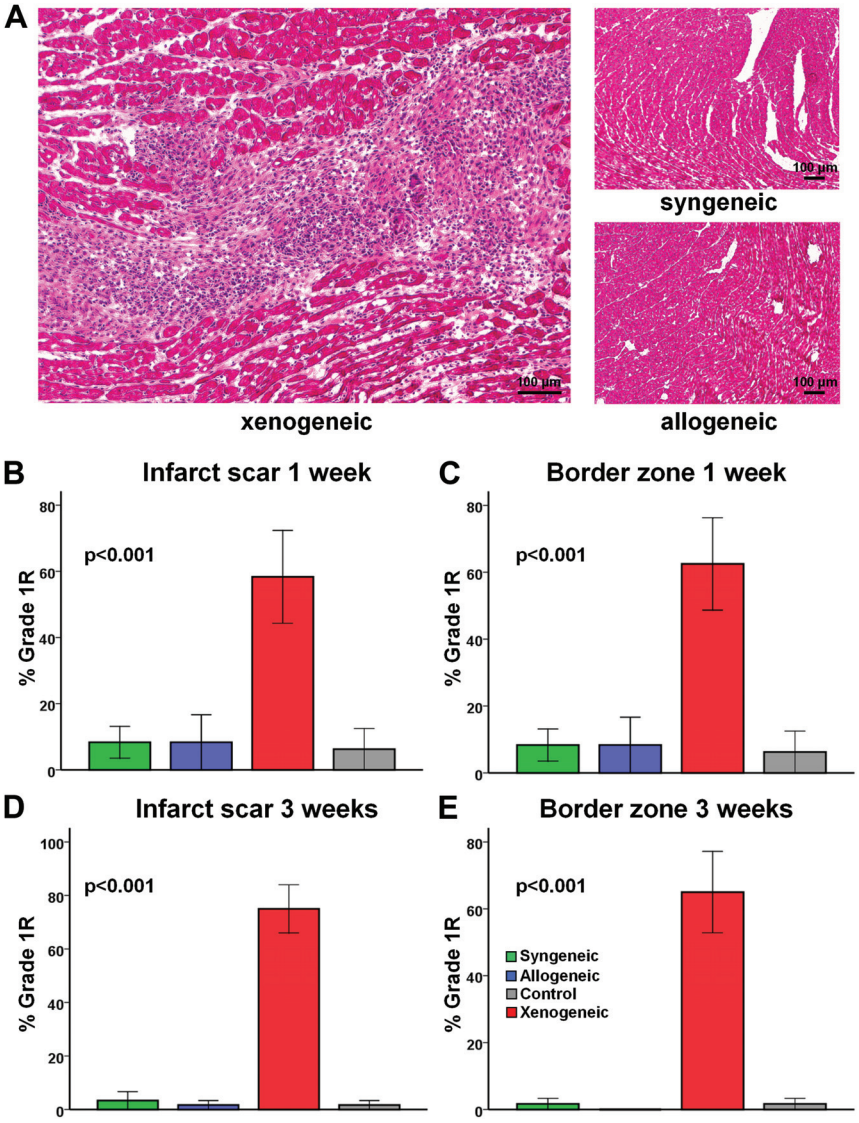

Figure 5. Assessment of local immune rejection by hematoxylin and eosin (H&E) staining. **A**, Representative images of H&E-stained heart sections. No immune reaction can be detected in the allogeneic setting, whereas perivascular and interstitial mononuclear infiltration with no foci of myocyte damage can be observed in the xenogeneic setting (grade 1R rejection). **B** through **E**, Quantitative analysis of immune rejection based on the International Society of Heart and Lung Transplantation (ISHLT) grading system demonstrated that no significant immune rejection could be detected in the infarct scar and border zone 1 or 3 weeks after allogeneic cell transplantation. In contrast, xenogeneic cell transplantation resulted in grade 1R rejection (n=4–5 per group at each time point).

planted cells. It is plausible that antigens shed by apoptotic donor CDCs are phagocytosed by host antigen-presenting cells (eg, dendritic cells) and subsequently presented to $CD4^+$ cells, thus activating the immune cascade; however, a role for the direct pathway of allorecognition cannot be ruled out.[13] Importantly, the increased lymphohistiocytic infiltration observed at 3 weeks was much lower than that seen with xenogeneic transplantation (Figure 6D) and had completely subsided by 6 months (Figure IV and Table VII in the online-only Data Supplement). The higher infiltration of macrophages (which did not localize within the infiltrates but were evenly dispersed along the infarct) detected at 1 and 3 weeks after MI in the xenogeneic and control groups was consistent with the larger infarct size observed in those groups.

To assess the possibility of systemic immunogenicity of CDC transplantation, levels of circulating inflammatory cytokines were measured in rat serum samples obtained 3 weeks after treatment. Quantification of inflammatory cytokines demonstrated comparable levels of circulating proinflammatory (IFN-γ, tumor necrosis factor-α, IL-1b, KC/GRO) and antiinflammatory (IL-5, IL-13, IL-4) cytokines in the syngeneic, allogeneic, and control groups. Conversely, in the xenogeneic setting, the circulating levels of IFN-γ, IL-1β, IL-13, and IL-4 were markedly increased (Figure I in the online-only Data Supplement). Taken together, these data indicate that the systemic inflammatory response observed after xenogeneic transplantation did not occur in the allogeneic setting.

Allogeneic CDCs Elicit a Cellular But Not a Humoral Immune Memory Response

To assess the development of cellular memory immune response after allogeneic CDC transplantation, the alloreactivity of lymphocytes isolated from spleens of allogeneic recipients 3 weeks after transplantation was assessed by 1-way mixed-lymphocyte reactions. Lymphocytes from sensitized animals exhibited higher proliferation after coculture with allogeneic CDCs compared with naïve lymphocytes or syngeneic cocultures (Figure IIIA and IIIB in the online-only Data Supplement). In addition, supernatant levels of inflammatory cytokines were markedly increased in the sensitized lymphocyte cocultures (Figure IIIC in

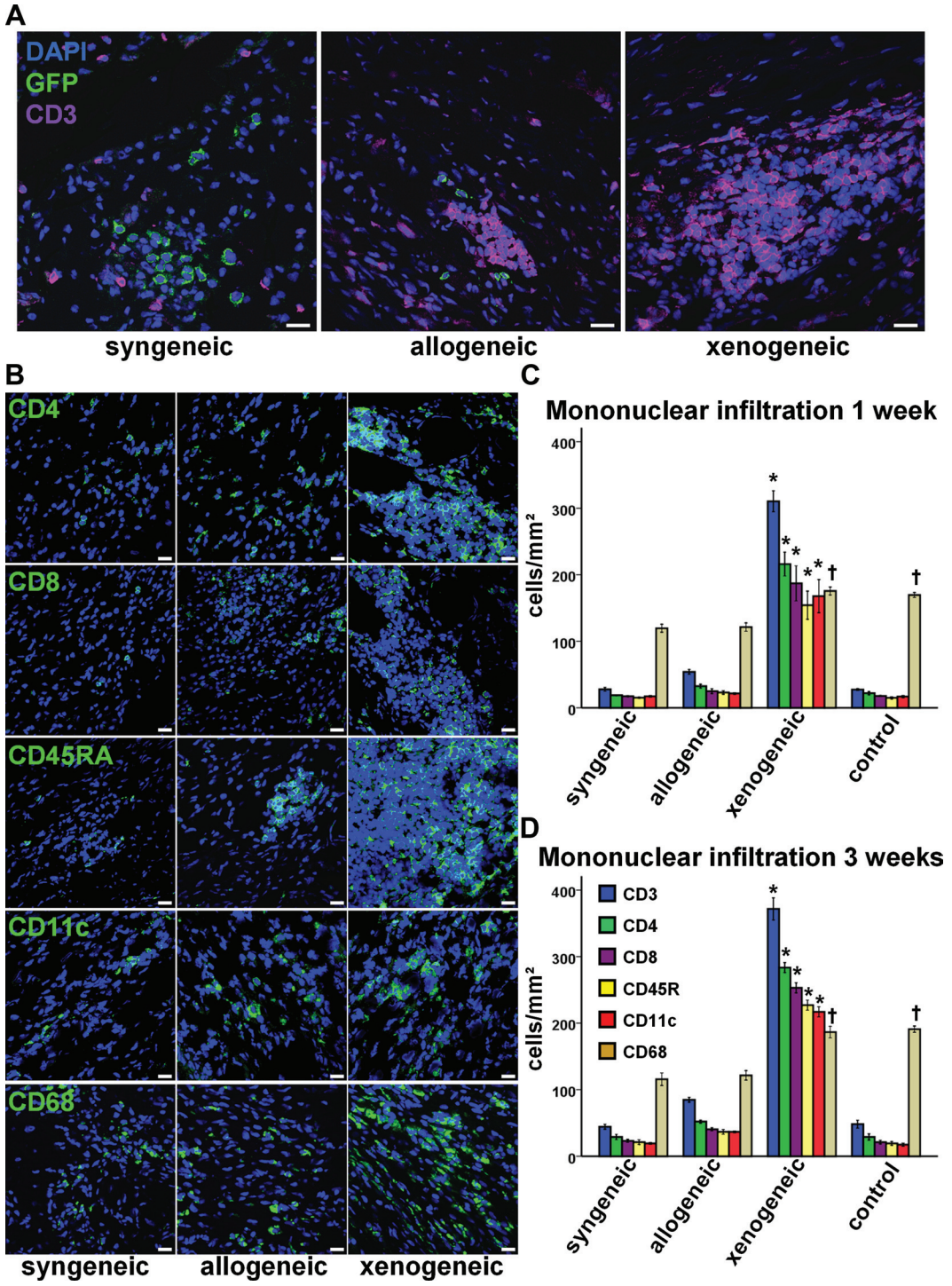

Figure 6. Assessment of local immune rejection by immunohistochemistry. **A** and **B**, Immunohistochemistry revealed small, sparse interstitial infiltrates in the proximity of some allogeneic cardiosphere-derived cells (CDCs) 3 weeks after transplantation, whereas large infiltrates could be detected in the xenogeneic setting. Infiltrates comprised mainly $CD3^+$ T lymphocytes (with equal contributions of $CD8^+$ T cytotoxic and $CD4^+$ T helper subpopulations) and, to a lesser extent, $CD45RA^+$ B lymphocytes and $CD11c^+$ dendritic cells. $CD68^+$ macrophages did not localize within the infiltrates and were evenly dispersed along the infarct (scale bars=20 μm). Mononuclear infiltration was significantly higher in the xenogeneic group at 1 week (**C**; n=4 per group) and 3 weeks (**D**; n=4 per group) after transplantation (*$P<0.05$ vs syngeneic and control groups; †$P<0.05$ vs syngeneic and allogeneic groups). GFP indicates green fluorescent protein.

the online-only Data Supplement). These findings, indicative of a T-cell memory response, are in accordance with the immunohistochemistry data showing a predominant role of T cells in the sparse mononuclear infiltrates observed 3 weeks after allogeneic transplantation (Figure 6C and 6D). We did not test whether the intensity of the cellular memory response diminishes with time, as reported in studies of allogeneic mesenchymal cell transplantation.[14]

To assess the development of a humoral memory response, recipient rat sera obtained 1 and 3 weeks after transplantation

were screened for circulating anti-donor antibodies. No alloreactive antibodies could be detected in any recipients of allogeneic CDCs at any time point. In contrast, in the xenogeneic setting, high titers of xenoreactive IgM antibodies were detected 1 and 3 weeks after transplantation, whereas a progressive increase in xenoreactive IgG antibodies was observed from week 1 to 3 (Figure II in the online-only Data Supplement). The development of anti-donor antibodies in xenogeneic but not allogeneic recipients is consistent with the ≈8-fold-higher B-cell myocardial infiltration observed in the xenogeneic setting (Figure 6C and 6D).

Allogeneic CDCs Promote Endogenous Cardiac Regeneration

To investigate the mechanisms of benefit, we examined the fate of transplanted cells. Immunohistochemistry revealed that syngeneic and allogeneic CDCs resided primarily in the border zone and infarct scar; a subset of cells were found to be cycling in vivo 1 and 3 weeks after MI, as indicated by Ki-67 positivity and BrdU incorporation (Figure V in the online-only Data Supplement). Rare events of cardiomyogenic (GFP^+/α-Sarcomeric Actinin $(\alpha SA)^+$ cells) and angiogenic (GFP^+/von Willebrand $factor^+$ cells) differentiation of surviving CDCs could be detected in both the syngeneic and the allogeneic setting. Although most $GFP^+/\alpha SA^+$ cells were small and exhibited an immature cardiomyocyte phenotype (Figure 7A), mature $GFP^+/\alpha SA^+$ cells structurally integrated into the host myocardium were occasionally seen (Figure 7B). In addition, GFP^+/von Willebrand $factor^+$ were found to be incorporated in microvessels in the risk region (Figure 7C). These observations, which confirm previous reports,[7,9,15] demonstrate the multilineage potential of CDCs. However, these needle in the haystack instances of direct differentiation are likely too low to account for the observed robust functional benefit.

We thus attempted to quantify endogenous cardiac regeneration. Possible mechanisms include upregulation of cycling cardiomyocytes (arising either from resident cardiomyocyte cell cycle reentry[16] or from differentiation of endogenous stem cells[17]), recruitment of endogenous progenitor cells to the site of cell transplantation,[6,17,18] and enhanced angiogenesis.[19] We found that syngeneic and allogeneic CDC therapy markedly enhanced the number of cycling host cardiomyocytes ($GFP^-/\alpha SA^+/Ki\text{-}67^+$ and $GFP^-/\alpha SA^+/BrdU^+$ cells; Figure 7D, 7E, 7G, and 7H) 1 and 3 weeks after MI. However, the number of cycling host cardiomyocytes significantly decreased from 1 to 3 weeks, dropping to nearly undetectable levels at 6 months. Syngeneic and allogeneic CDC transplantation also recruited endogenous stem cells (Figure 7F and 7I); the number of $GFP^-/c\text{-}Kit^+$ cells was increased in CDC-treated hearts compared with controls at 1 and 3 weeks after MI. As with resident cycling myocytes, the number of endogenous progenitors decreased as a function of time after treatment.

Finally, syngeneic and allogeneic CDC transplantation enhanced angiogenesis in the infarct border zone. Vessel density, identified by immunostaining for von Willebrand factor, was markedly increased 3 weeks after cell therapy compared with controls (Figure 7J and 7K). It should be noted that these endogenous reparative mechanisms were also mobilized in the control hearts. However, their magnitude was amplified (to similar degrees) by syngeneic and allogeneic CDC therapy.

Taken together, these data indicate that exogenous CDC administration stimulates activation of endogenous repair and regeneration pathways, confirming previous studies[5,6] reporting that the majority of the observed benefit after cell therapy is attributable to indirect mechanisms rather than differentiation of transplanted cells. We thus quantified myocardial levels of beneficial paracrine factors in the infarct border zone. Western blot analysis revealed increased secretion of vascular endothelial growth factor, insulin-like growth factor-1, and hepatocyte growth factor in hearts treated with syngeneic and allogeneic CDCs compared with controls at days 1, 4, and 7 after MI (Figure 8A–8D). On the contrary, rats treated with xenogeneic CDCs had increased myocardial levels of these cytokines only at 1 day after MI, not at later time points (Figure VI in the online-only Data Supplement). Three weeks after MI, no difference could be observed among groups. The data reveal that syngeneic and allogeneic CDCs are equivalent in their paracrine benefits, in both magnitude and time course, and that sustained increased levels of vascular endothelial growth factor, insulin-like growth factor-1, and hepatocyte growth factor, at least during the first week after cell transplantation, underlie the functional benefit. Our experimental design (transplantation of rCDCs into rat hearts and the use of antibodies that detect both human and rat cytokine isoforms) cannot elucidate whether the increased myocardial levels of these factors are attributable to direct secretion by transplanted cells, upregulation of host tissue humoral responses,[20] or both. Nevertheless, prior work shows that the release of paracrine factors directly from CDCs is substantial in the early posttransplantation period.[5]

Discussion

We report a detailed spatiotemporal evaluation of the local and systemic immune responses after allogeneic CDC transplantation for myocardial repair. Allogeneic CDC transplantation without immunosuppression is safe and produces structural and functional benefits after MI by stimulating endogenous cardiac regeneration. This indirect mechanism of action, shared by syngeneic cells, explains why benefits persist despite the temporary engraftment of transplanted cells.

CDCs represent an attractive cell type for heart repair and regeneration. CDCs are clonogenic and exhibit multilineage potential, thus fulfilling key criteria for heart-derived stem cells.[15] Over the past 6 years, we have demonstrated that CDCs can improve cardiac function after MI in mice,[5,7,21] rats,[9,22,23] and pigs.[24,25] Importantly, several independent laboratories worldwide have reproduced the published methodology and verified the identity and utility of CDCs.[26–32] On the other hand, critiques of the cardiosphere methodology have appeared,[33,34] but as we have pointed out in detailed rebuttals,[8,15] these studies did not follow published protocols for CDC isolation and expansion, and the methodological variations likely explain the negative results. With regard to

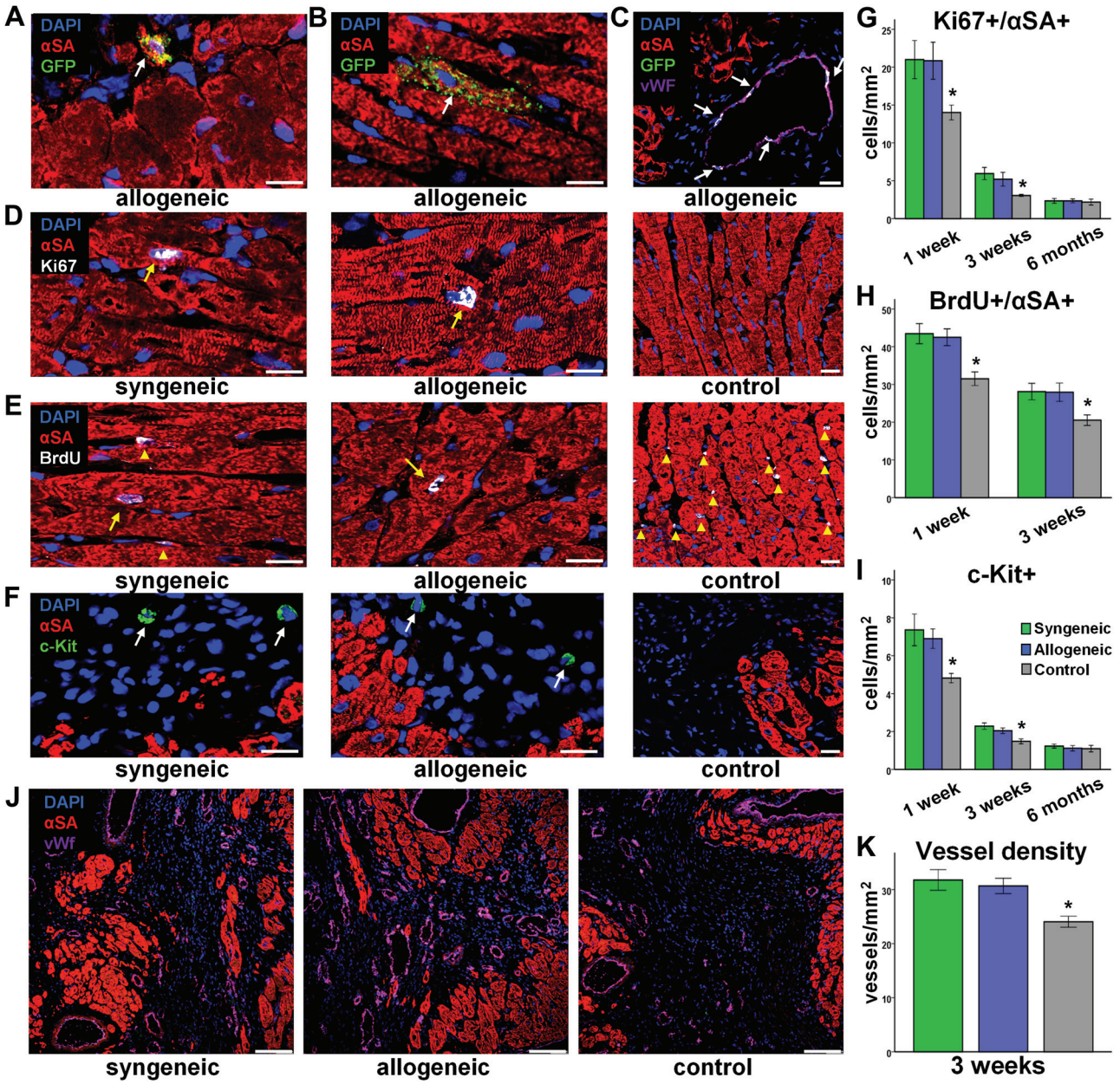

Figure 7. Direct and indirect contributions of allogeneic cardiosphere-derived cells (CDCs) to myocardial repair. Rare events of long-term engraftment and cardiogenic (**A** and **B**) or angiogenic (**C**) differentiation of allogeneic CDCs could be detected. More important, syngeneic and allogeneic CDCs promoted endogenous mechanisms of regeneration by stimulating cardiomyocyte cycling (**D**, **E**, **G**, and **H**; n=5–8 per group at each time point), host stem cell recruitment (**F** and **I**; n=5–8 per group at each time point), and angiogenesis (**J** and **K**; n=8 per group; **P*<0.05 vs syngeneic and allogeneic groups). Arrows in **D** and **E** denote cardiomyocyte nuclei and arrowheads denote noncardiomyocyte nuclei; arrows in **F** denote c-Kit$^+$ cells. **A** through **F,** scale bars=20 μm; **J** and **K,** scale bars=100 μm). GFP indicates green fluorescent protein; αSA, α-Sarcomeric Actinin; vWf, von Willebrand factor.

clinical translation, highly positive results from a proof-of-concept clinical study using autologous CDCs, the CArdiosphere-Derived aUtologous stem CElls to reverse ventricULar dySfunction (CADUCEUS; NCT00893360[3]) trial, have recently been reported.[35]

The avoidance of immunologic rejection renders autologous therapy attractive, but serious disadvantages dampen enthusiasm. Patient-specific tissue harvesting and cell processing result in a delay to therapy and introduce possible variations in cell potency related to patient age and disease.[4] Here, we tested the specific hypothesis that allogeneic CDCs are hypoimmunogenic in vivo and can survive in the infarcted myocardium for a critical period of time to stimulate endogenous reparative and regenerative pathways, resulting in sustained benefit. We found that allogeneic CDC transplantation without immunosuppression induces only a transient mild local immune reaction in a rat MI model. In the clinical setting, development of an immune response after allogeneic CDC delivery to the heart could theoretically lead to immune-related myocardial damage (which, on the basis of our findings, would be unlikely because no foci of myocardial damage were detected even after xenogeneic CDC transplan-

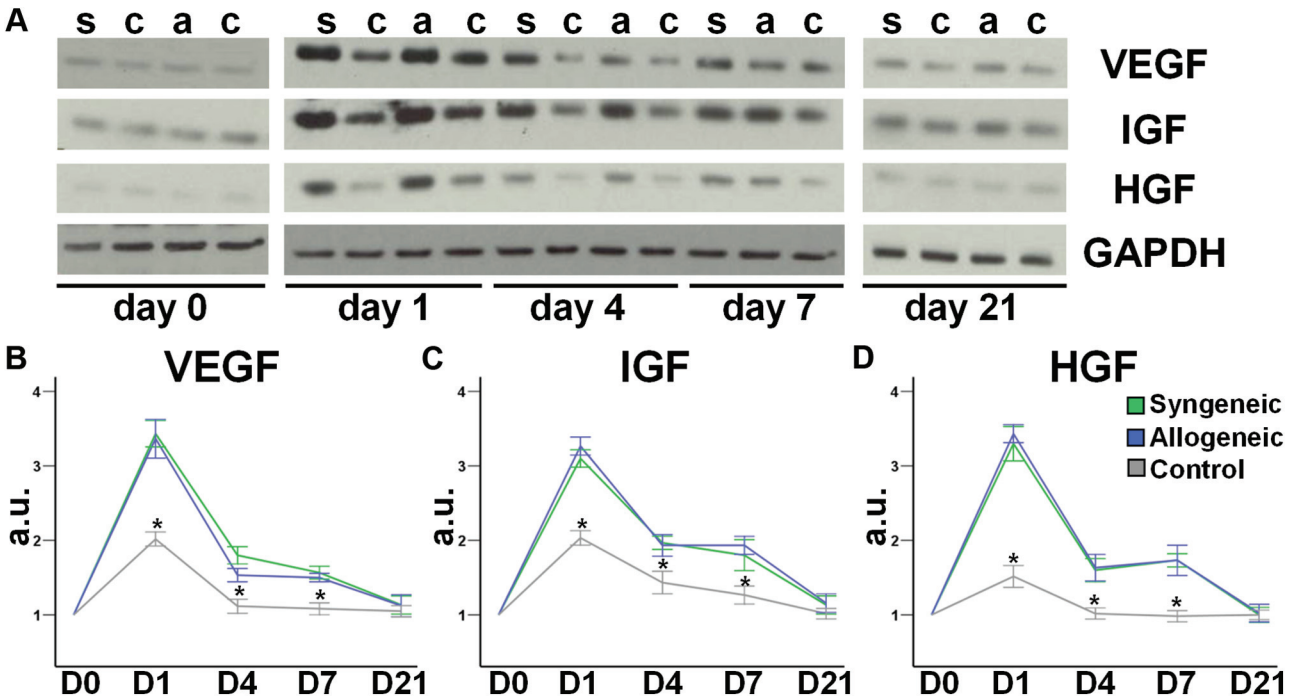

Figure 8. Detection of beneficial paracrine factors by Western blotting. **A**, Representative blots demonstrating increased secretion of vascular endothelial growth factor (VEGF), insulin-like growth factor (IGF-1), and hepatocyte growth factor (HGF) during the first week after syngeneic (s) and allogeneic (a) cardiosphere-derived cell (CDC) transplantation. Quantitative analysis of myocardial levels of VEGF (**B**), IGF-1 (**C**), and HGF (**D**) after myocardial infarction (n=4–6 per group at each time point; *$P<0.05$ vs syngeneic and allogeneic groups). a.u. Indicates arbitrary unit; c, control.

tation) and allosensitization of the cell recipient, which in turn could complicate repeat dosing with the same batch of cells (a problem that could easily be overcome by administering cells from different donors) and complicate future organ transplantation (if the CDC donor and organ donor share similar HLA haplotypes). We did not detect any circulating anti-donor antibodies after allogeneic CDC transplantation, implying that no significant increase in panel reactive antibodies would occur; the absence of such sensitization at baseline increases the likelihood of allograft survival.[36] In addition, the small inocula associated with CDC therapy (compared, for example, with the volumes used in blood transfusions) make sensitization of the recipient improbable. Nevertheless, the possibility of recipient allosensitization should be investigated in large animals as a prelude to studies in human subjects.

We have also shown that transient and rather paltry short-term cell survival suffices to produce dramatic lasting benefits. Despite lower cell engraftment, allogeneic CDC transplantation generates structural and functional benefits that are indistinguishable from syngeneic transplantation and persist 6 months after MI. The equivalence of allogeneic and syngeneic transplantation is not surprising once we recognize and accept the central paradox: Few, briefly present transplanted cells suffice to produce large, durable benefits by amplifying endogenous pathways of repair and regeneration rather than by directly generating new transplanted tissue. This indirect "amplifier effect," impressive as it may be, is not yet fully understood.[2] Even though we show that allogeneic CDCs stimulate host cardiomyocyte cycling, endogenous stem cell recruitment, and angiogenesis in the post-MI setting, it is unclear whether these phenomena can account for the totality of the observed benefit; other mechanisms could involve cytoprotection of the host tissue or modulation of inflammatory processes, resulting in better infarct healing. In addition, it is unclear how much of the benefit is attributable to the identified paracrine factors; insulin-like growth factor-1 and hepatocyte growth factor have been shown to mobilize resident cardiac stem cells,[37] whereas vascular endothelial growth factor is well known to stimulate angiogenesis.[38] Alternatively, other factors[39] may also play important roles. Identification of the appropriate cocktail of beneficial growth factors and incorporation into a formulation enabling sustained and controlled local release after cardiac delivery is a conceptually attractive approach. However, cell-mediated contact-dependent mechanisms may also contribute to the observed effects.[40]

Regardless of the mechanism, in practice, the present work opens up a new treatment paradigm: CDCs could be grown in large numbers from allogeneic heart tissue in a central facility under strict quality control and banked for future use, enabling safe and effective myocardial repair in a timely, cost-efficient manner. Potential sources of allogeneic heart tissue include hearts explanted from organ donors but not used for transplantation, cadaveric hearts from the recently deceased, and surgical discards. Hearts obtained from organ donors (but not used for transplantation) have the inherent advantage that donors are, by definition, healthy and have been previously HLA typed and screened for infectious diseases, with the tissue maintained viable and sterile until processed. Hearts from organ donors after cardiac death are particularly attractive because they are rarely used for trans-

plantation, although kidneys, liver, and pancreas are commonly used.[41] In 2008, there were 832 organ donors after cardiac death in the United States, and no hearts were used for cardiac transplantation[42]; these hearts represent one pool from which source tissue can be obtained for allogeneic CDC culture. Cadaveric hearts from healthy, noninfectious donors also could be used; however, the tissue is not optimally stored, and samples would have to be obtained with low postmortem intervals. Surgical discards are yet another source option; although these specimens are more abundant, donors are apt to have an existing cardiac disorder or other comorbidities (which may or may not hamper cell quality).

Conclusions

We demonstrate that allogeneic CDC transplantation without immunosuppression is safe, promotes cardiac regeneration, and improves heart function in a rat MI model, mainly through stimulation of endogenous repair mechanisms. This indirect mechanism of action rationalizes the lasting benefit brought about by ephemeral transplanted cells in that the new tissue originates from the recipient rather than the donor. This work motivates the testing of allogeneic hCDCs as a potential clinical product for cellular cardiomyoplasty.

Sources of Funding

This work was supported by the National Institutes of Health (R01 HL083109) and the Cedars-Sinai Board of Governors Heart Stem Cell Center. Dr E. Marbán holds the Mark S. Siegel Family Chair of the Cedars-Sinai Medical Center.

Disclosures

Drs E. Marbán and L. Marbán are founders and equity holders in Capricor, Inc. Dr L. Marbán receives salary from Capricor, Inc. Drs Malliaras and Terrovitis receive consulting fees from Capricor, Inc. The other authors report no conflicts.

References

1. Wollert KC, Drexler H. Cell therapy for the treatment of coronary heart disease: a critical appraisal. *Nat Rev Cardiol*. 2010;7:204–215.
2. Malliaras K, Marbán E. Cardiac cell therapy: where we've been, where we are, and where we should be headed. *Br Med Bull*. 2011;98:161–185.
3. CADUCEUS. CArdiosphere-Derived aUtologous stem CElls to reverse ventricULar dySfunction (NCT00893360). www.clinicaltrials.gov. Accessed November 17, 2011.
4. Dimmeler S, Leri A. Aging and disease as modifiers of efficacy of cell therapy. *Circ Res*. 2008;102:1319–1330.
5. Chimenti I, Smith RR, Li TS, Gerstenblith G, Messina E, Giacomello A, Marbán E. Relative roles of direct regeneration versus paracrine effects of human cardiosphere-derived cells transplanted into infarcted mice. *Circ Res*. 2010;106:971–980.
6. Tang XL, Rokosh G, Sanganalmath SK, Yuan F, Sato H, Mu J, Dai S, Li C, Chen N, Peng Y, Dawn B, Hunt G, Leri A, Kajstura J, Tiwari S, Shirk G, Anversa P, Bolli R. Intracoronary administration of cardiac progenitor cells alleviates left ventricular dysfunction in rats with a 30-day-old infarction. *Circulation*. 2010;121:293–305.
7. Smith RR, Barile L, Cho HC, Leppo MK, Hare JM, Messina E, Giacomello A, Abraham MR, Marbán E. Regenerative potential of cardiosphere-derived cells expanded from percutaneous endomyocardial biopsy specimens. *Circulation*. 2007;115:896–908.
8. Davis DR, Zhang Y, Smith RR, Cheng K, Terrovitis J, Malliaras K, Li TS, White A, Makkar R, Marbán E. Validation of the cardiosphere method to culture cardiac progenitor cells from myocardial tissue. *PLoS One*. 2009;4:e7195.
9. Cheng K, Li TS, Malliaras K, Davis DR, Zhang Y, Marbán E. Magnetic targeting enhances engraftment and functional benefit of iron-labeled cardiosphere-derived cells in myocardial infarction. *Circ Res*. 2010;106:1570–1581.
10. Ruggeri L, Capanni M, Martelli MF, Velardi A. Cellular therapy: exploiting NK cell alloreactivity in transplantation. *Curr Opin Hematol*. 2001;8:355–359.
11. Atoui R, Shum-Tim D, Chiu RC. Myocardial regenerative therapy: immunologic basis for the potential "universal donor cells." *Ann Thorac Surg*. 2008;86:327–334.
12. Terrovitis J, Stuber M, Youssef A, Preece S, Leppo M, Kizana E, Schär M, Gerstenblith G, Weiss RG, Marbán E, Abraham MR. Magnetic resonance imaging overestimates ferumoxide-labeled stem cell survival after transplantation in the heart. *Circulation*. 2008;117:1555–1562.
13. Kreisel D, Krupnick AS, Gelman AE, Engels FH, Popma SH, Krasinskas AM, Balsara KR, Szeto WY, Turka LA, Rosengard BR. Non-hematopoietic allograft cells directly activate CD8+ T cells and trigger acute rejection: an alternative mechanism of allorecognition. *Nat Med*. 2002;8:233–239.
14. Poncelet AJ, Vercruysse J, Saliez A, Gianello P. Although pig allogeneic mesenchymal stem cells are not immunogenic in vitro, intracardiac injection elicits an immune response in vivo. *Transplantation*. 2007;83:783–790.
15. Davis DR, Ruckdeschel Smith R, Marbán E. Human cardiospheres are a source of stem cells with cardiomyogenic potential. *Stem Cells*. 2010;28:903–904.
16. Bersell K, Arab S, Haring B, Kühn B. Neuregulin1/ErbB4 signaling induces cardiomyocyte proliferation and repair of heart injury. *Cell*. 2009;138:257–270.
17. Loffredo FS, Steinhauser ML, Gannon J, Lee RT. Bone marrow-derived cell therapy stimulates endogenous cardiomyocyte progenitors and promotes cardiac repair. *Cell Stem Cell*. 2011;8:389–398.
18. Hatzistergos KE, Quevedo H, Oskouei BN, Hu Q, Feigenbaum GS, Margitich IS, Mazhari R, Boyle AJ, Zambrano JP, Rodriguez JE, Dulce R, Pattany PM, Valdes D, Revilla C, Heldman AW, McNiece I, Hare JM. Bone marrow mesenchymal stem cells stimulate cardiac stem cell proliferation and differentiation. *Circ Res*. 2010;107:913–922.
19. Kamihata H, Matsubara H, Nishiue T, Fujiyama S, Tsutsumi Y, Ozono R, Masaki H, Mori Y, Iba O, Tateishi E, Kosaki A, Shintani S, Murohara T, Imaizumi T, Iwasaka T. Implantation of bone marrow mononuclear cells into ischemic myocardium enhances collateral perfusion and regional function via side supply of angioblasts, angiogenic ligands, and cytokines. *Circulation*. 2001;104:1046–1052.
20. Cho HJ, Lee N, Lee JY, Choi YJ, Ii M, Wecker A, Jeong JO, Curry C, Qin G, Yoon YS. Role of host tissues for sustained humoral effects after endothelial progenitor cell transplantation into the ischemic heart. *J Exp Med*. 2007;204:3257–3269.
21. Li TS, Cheng K, Lee ST, Matsushita S, Davis D, Malliaras K, Zhang Y, Matsushita N, Smith RR, Marbán E. Cardiospheres recapitulate a niche-like microenvironment rich in stemness and cell-matrix interactions, rationalizing their enhanced functional potency for myocardial repair. *Stem Cells*. 2010;28:2088–2098.
22. Davis DR, Kizana E, Terrovitis, Barth AS, Zhang Y, Smith RR, Miake J, Marbán E. Isolation and expansion of functionally-competent cardiac progenitor cells directly from heart biopsies. *J Mol Cell Cardiol*. 2010;49:312–321.
23. Terrovitis J, Lautamäki R, Bonios, Fox J, Engles JM, Yu J, Leppo MK, Pomper MG, Wahl RL, Seidel J, Tsui BM, Bengel FM, Abraham MR, Marbán E. Noninvasive quantification and optimization of acute cell retention by in vivo positron emission tomography after intramyocardial cardiac-derived stem cell delivery. *J Am Coll Cardiol*. 2009;54:1619–1626.
24. Lee ST, White AJ, Matsushita, Malliaras K, Steenbergen C, Zhang Y, Li TS, Terrovitis J, Yee K, Simsir S, Makkar R, Marbán E. Intramyocardial injection of autologous cardiospheres or cardiosphere-derived cells preserves function and minimizes adverse ventricular remodeling in pigs with heart failure post-myocardial infarction. *J Am Coll Cardiol*. 2011;57:455–465.
25. Johnston PV, Sasano T, Mills, Evers R, Lee ST, Smith RR, Lardo AC, Lai S, Steenbergen C, Gerstenblith G, Lange R, Marbán E. Engraftment, differentiation, and functional benefits of autologous cardiosphere-derived cells in porcine ischemic cardiomyopathy. *Circulation*. 2009;120:1075–1083.
26. Aghila Rani KG, Kartha CC. Effects of epidermal growth factor on proliferation and migration of cardiosphere-derived cells expanded from adult human heart. *Growth Factors*. 2010;28:157–165.
27. Gaetani R, Ledda M, Barile L, Chimenti I, De Carlo F, Forte E, Ionta V, Giuliani L, D'Emilia E, Frati G, Miraldi F, Pozzi D, Messina E, Grimaldi S, Giacomello A, Lisi A. Differentiation of human adult cardiac stem

cells exposed to extremely low-frequency electromagnetic fields. *Cardiovasc Res*. 2009;82:411–420.
28. Mishra R, Vijayan K, Colletti E, Harrington DA, Matthiesen TS, Simpson D, Goh SK, Walker BL, Almeida-Porada G, Wang D, Backer CL, Dudley SC Jr, Wold LE, Kaushal S. Characterization and functionality of cardiac progenitor cells in congenital heart patients. *Circulation*. 2011;123:364–373.
29. Takehara N, Tsutsumi Y, Tateishi, Ogata T, Tanaka H, Ueyama T, Takahashi T, Takamatsu T, Fukushima M, Komeda M, Yamagishi M, Yaku H, Tabata Y, Matsubara H, Oh H. Controlled delivery of basic fibroblast growth factor promotes human cardiosphere-derived cell engraftment to enhance cardiac repair for chronic myocardial infarction. *J Am Coll Cardiol*. 2008;52:1858–1865.
30. Tang YL, Zhu W, Cheng, Chen L, Zhang J, Sun T, Kishore R, Phillips MI, Losordo DW, Qin G. Hypoxic preconditioning enhances the benefit of cardiac progenitor cell therapy for treatment of myocardial infarction by inducing CXCR4 expression. *Circ Res*. 2009;104:1209–1216.
31. Zakharova L, Mastroeni D, Mutlu N, Molina M, Goldman S, Diethrich E, Gaballa MA. Transplantation of cardiac progenitor cell sheet onto infarcted heart promotes cardiogenesis and improves function. *Cardiovasc Res*. 2010;87:40–49.
32. Koninckx R, Daniëls A, Windmolders S, Carlotti F, Mees U, Steels P, Rummens JL, Hendrikx M, Hensen K. Mesenchymal stem cells or cardiac progenitors for cardiac repair? A comparative study. *Cell Mol Life Sci*. 2011;68:2141–2156.
33. Andersen DC, Andersen P, Schneider M, Jensen HB, Sheikh SP. Murine "cardiospheres" are not a source of stem cells with cardiomyogenic potential. *Stem Cells*. 2009;27:1571–1581.
34. Shenje LT, Field LJ, Pritchard C, Guerin CJ, Rubart M, Soonpaa MH, Ang KL, Galiñanes M. Lineage tracing of cardiac explant derived cells. *PLoS One*. 2008;3:e1929.
35. Makkar R, Smith RR, Cheng K, Malliaras K, Thomson LE, Berman DS, Czer L, Marbán L, Mendizabal A, Johnston PV, Russell S, Schuleri KH, Lardo AC, Gerstenblith G, Marbán E. The CADUCEUS (CArdiosphere-Derived aUtologous stem CElls to reverse ventricULar dySfunction) Trial [abstract]. http://my.americanheart.org/professional/Sessions/ScientificSessions/ScienceNews/SS11-Clinical-Science-Special-Reports_UCM_433393_Article.jsp. Accessed November 17, 2011.
36. Lefaucheur C, Suberbielle-Boissel C, Hill GS, Nochy D, Andrade J, Antoine C, Gautreau C, Charron D, Glotz D. Clinical relevance of preformed HLA donor-specific antibodies in kidney transplantation. *Am J Transplant*. 2008;8:324–331.
37. Linke A, Muller P, Nurzynska D, Casarsa C, Torella D, Nascimbene A, Castaldo C, Cascapera S, Bohm M, Quaini F, Urbanek K, Leri A, Hintze TH, Kajstura J, Anversa P. Stem cells in the dog heart are self-renewing, clonogenic, and multipotent and regenerate infarcted myocardium, improving cardiac function. *Proc Natl Acad Sci U S A*. 2005;102:8966–8971.
38. Gnecchi M, Zhang Z, Ni A, Dzau VJ. Paracrine mechanisms in adult stem cell signaling and therapy. *Circ Res*. 2008;103:1204–1219.
39. Stastna M, Chimenti I, Marbán E, Van Eyk JE. Identification and functionality of proteomes secreted by rat cardiac stem cells and neonatal cardiomyocytes. *Proteomics*. 2010;10:245–253.
40. Xie Y, Cheng K, Cho HC, Malliaras K, Ibrahim A, Sun B, Galang G, Ionta V, Shen D, Zhang Y, Marban E. Human Cardiosphere-Derived Cells Stimulate Cardiomyocyte Proliferation in vivo and in Co-Culture [abstract]. *Circulation*. 2011;124:A16688.
41. Steinbrook R. Organ donation after cardiac death. *N Engl J Med*. 2007;357:209–213.
42. The 2009 annual report of the OPTN and SRTR: transplant data 1999–2008. www.ustransplant.org. Accessed November 17, 2011.

CLINICAL PERSPECTIVE

Cardiosphere-derived cells (CDCs) are an attractive cell type for cardiomyoplasty after myocardial infarction, and autologous CDCs are already being tested clinically in the CArdiosphere-Derived aUtologous stem CElls to reverse ventricULar dySfunction (CADUCEUS) trial. Autologous therapy avoids immunologic rejection but necessitates patient-specific tissue harvesting, cell processing, and quality control, resulting in 3- to 6-week delays to therapy and possible variations in cell potency related to patient age and comorbidities. The use of universal donor (allogeneic) cells, if safe and effective, would obviate such limitations; however, immune rejection may limit effectiveness regardless of whether it poses safety hazards. Thus, we compared syngeneic and allogeneic CDC transplantation in infarcted rats from immunologically mismatched inbred strains. We demonstrate that allogeneic CDC therapy without immunosuppression is safe and induces only a mild transient local response without signs of systemic immunogenicity. Despite lower long-term engraftment compared with syngeneic cells, allogeneic CDCs produce similar structural and functional beneficial effects (which persist at least 6 months after transplantation). The benefits are due to stimulation of endogenous repair mechanisms and regrowth of recipient heart tissue rather than formation of new donor-derived myocardium. In practice, the present work opens up a new treatment paradigm: CDCs could be grown in large numbers from allogeneic heart tissue in a central facility under strict quality control and banked for future use, enabling safe and effective myocardial repair in a timely, cost-efficient manner. This work motivates the testing of allogeneic human CDCs as a potential clinical product for cellular cardiomyoplasty.

SUPPLEMENTAL MATERIAL

Supplemental Methods

Cell culture

Rat CDCs (rCDCs) were expanded from explanted hearts obtained from 8-week old male WKY rats. Human CDCs (hCDCs) were expanded from human endomyocardial biopsies or myocardial samples, obtained from adult male patients during clinically-indicated procedures after informed consent, under a protocol approved by the Institutional Review Board. The myocardial specimens (both rat hearts and human biopsies) were cut into fragments less than 1 mm^3, washed and partially digested with trypsin (0.05%; GIBCO). These tissue fragments were culture as cardiac explants on fibronectin (20 mg/ml; Sigma) coated dishes in cardiac explant media [CEM; Iscove's Modified Dulbecco's Medium (GIBCO), fetal bovine serum 20% (HyClone, Logan, UT), 100 U/ml penicillin G (GIBCO), 100 U/ml streptomycin (GIBCO), and 0.1 mmol/l 2-mercaptoethanol (GIBCO)]. After a variable period of growth, a layer of stromal-like cells emerged from the cardiac explant over which phase bright cells proliferated. The loosely-adherent cells surrounding the explant (termed cardiac outgrowth) were harvested using mild enzymatic digestion (0.05% trypsin under direct visualization, GIBCO). Cardiac outgrowth could be harvested up to four more times from the same specimen. Harvested cardiac outgrowth was seeded at 50,000 cells/ml on poly-D-lysine coated dishes in CEM. Several days later, cells that remained adherent to the poly-D-lysine coated dishes were discarded, while free-floating cardiospheres were harvested, plated on fibronectin coated flasks and cultured in CEM to generate CDCs.

Flow cytometry

Flow cytometry experiments were performed in order to evaluate surface expression of MHC class I, MHC class II and costimulatory molecules (CD 80, CD86) in human and rat CDCs, both under baseline conditions and after stimulation with 100 ng/ml interferon-γ for 1 day and 7 days. In addition, general phenotypic characterization of CDCs (expression of CD105, c-Kit, CD90, CD31, CD45, CD140b, Discoidin domain-containing receptor 2 [DDR2] and α-smooth muscle actin) was performed. The antibodies are listed in supplemental table 3. Experiments were performed using a benchtop flow cytometer (FACSCalibur; BD Biosciences, San Jose, Ca). Gates were established by 7-amino-actinomycin D fluorescence and forward scatter to exclude dead cells. Fluorescent compensation was performed using single labeled controls. The percentage of positive cells was defined as the percent of the population falling above the 99th percentile of an isotype-matched antibody control cell population. Quantitative analysis was performed using CellQuest software (BD Biosciences).

Mixed-lymphocyte reaction

In order to assess the in vitro immunogenicity of CDCs, one-way mixed lymphocyte reactions were performed. Lymphocytes were isolated from euthanized WKY and BN rat spleens using standard protocols. In brief, spleens were harvested aseptically, mechanically dissociated and filtered through a 100 µm nylon mesh. Erythrocytes were lysed with 0.83% ammonium chloride, cells were washed in RPMI 1640, dead cells were removed by density centrifugation and cell viability was assessed by trypan blue dye exclusion. Stimulating rCDCs and hCDCs were mitotically inactivated with 50 µg/ml mitomycin C (Sigma-Aldrich) in the dark at 37°C for 30 minutes and washed three times with RPMI 1640. 10^4 stimulating CDCs were cocultured with 10^5 responder lymphocytes in 200 µl of culture medium (RPMI 1640 supplemented with 10%

FBS) in 96-well flat-bottom plates for 5 days. The following experimental conditions were tested in quadruplicates: a) rCDCs cocultured with WKY lymphocytes (syngeneic coculture); b) rCDCs cocultured with BN lymphocytes (allogeneic coculture); c) hCDCs cocultured with BN lymphocytes (xenogeneic coculture). All appropriate controls were also tested. BrdU was added to the cocultures for the last 24 hours and responder cell proliferation was assessed by the Cell Proliferation Biotrak ELISA System (GE Healthcare) according to the manufacturer's instructions. Absorbance was measured with a microplate reader (Bio-Rad) at 450 nm. Alloreactive and xenoreactive lymphocyte proliferation is presented as relative proliferative response, normalized to syngeneic coculture proliferation (stimulation index). The cell-free supernatant of the cocultures was collected and the levels of secreted IFN-g, IL-1b, IL-13, IL-4, IL-5, KC/GRO and TNF-a were measured by electrochemiluminescence. The levels of secreted IL-2 were measured using enzyme-linked immunosorbent assay (ELISA) kits, according to the manufacturer's protocols (R&D Systems)

Myocardial infarction and cell injection

Female WKY and BN rats (8-10 week old) underwent left thoracotomy under general anesthesia with 2% isoflurane. MI was produced by permanent ligation of the left anterior descending coronary artery. CDCs (2 million, suspended in120 μl of phosphate-buffered saline [PBS]) or vehicle were intramyocardially injected with a 29-gauge needle at 4 sites along the periphery of the infarct. The following experimental conditions were tested: a) injection of rCDCs into infarcted hearts of WKY rats (syngeneic group); b) injection of rCDCs into infarcted hearts of BN rats (allogeneic group); c) injection of hCDCs into infarcted hearts of BN rats (xenogeneic group); d) a) injection of vehicle into infarcted hearts of WKY rats (control group a); e) injection of vehicle into infarcted hearts of BN rats (control group b). 2 control groups were used in order

to confirm that both strains of rats respond similarly to myocardial infarction. After injections were completed, the chest was closed, anesthesia was discontinued and the animals were allowed to recover. In order to monitor proliferation of both transplanted and endogenous cells, subset of animals was intraperitoneally-injected with BrdU (100mg/kg body weight) daily for either the first week or the second and third week post MI.

Echocardiography

Echocardiography was performed to assess global cardiac function 6 hours (baseline), 3 weeks, 3 months and 6 months after surgery, using the Vevo 770 Imaging System (VISUALSONICS, Toronto, Canada). After the induction of general anesthesia with 2% isoflurane, the hearts were imaged two-dimensionally in the long-axis view (at the level of the greatest LV diameter) and in the short-axis view (at the level of the papillary muscle). Fractional area change (FAC) and left ventricular ejection fraction (LVEF) were measured from the long-axis view while fractional shortening (FS) was measured from the M-mode of the short axis view with Visual Sonics V1.3.8 software.

Quantification of engraftment by real time PCR

Quantitative PCR was performed 1 week and 3 weeks post cell injection in order to monitor transplanted cell survival after syngeneic, allogeneic and xenogeneic cell transplantation. We injected cells isolated from male donor WKY rats and male humans in the myocardium of female recipients and quantified absolute cell engraftment by real-time PCR using the (rat and human respectively) SRY gene located on the Y chromosome as target. In brief, the recipient heart was explanted, weighted, homogenized and genomic DNA was isolated using the DNA

Easy minikit (Qiagen), according to the manufacturer's protocol. The TaqMan® assay (Applied Biosystems) was used to quantify the number of transplanted cells with the rat (for syngeneic and allogeneic transplantation) and human (for xenogeneic transplantation) SRY gene as template. A standard curve was constructed with samples derived from multiple log dilutions of genomic DNA, isolated from male rat hearts and samples of male human myocardium, spiked with 50ng of female rat genomic DNA as control. The copy number of the SRY gene at each point of the standard curve was calculated based on the amount of DNA in each sample and the total mass of the rat genome per diploid cell. All samples were tested in triplicates. For each reaction, 50ng of template DNA was used. Real time PCR was performed in an ABI PRISM 7700 instrument. The result from each reaction, copies of the SRY gene in 50ng of genomic DNA, was expressed as the number of engrafted cells/heart by extrapolation to the total DNA content of each heart, taking into account that there is one copy of the SRY gene per transplanted cell.

Histology

Rats were sacrificed 1 week, 3 weeks and 6 months after treatment. Hearts were arrested with KCl solution, explanted, frozen in OCT compound, and sectioned in 5 μm sections on a cryostat. Cryosections were subsequently fixed with 4% paraformaldehyde. Quantitative morphometric analysis with Masson's trichrome staining (6 sections per heart, collected at 400 μm intervals) was performed to examine scar size, infarcted wall thickness and LV remodeling as described previously. In order to evaluate immune rejection, sections (12 sections per heart, collected at 200 μm intervals) were stained with hematoxylin and eosin and evaluated by a blinded cardiac pathologist; in addition immunostaining against immune cell markers (12 sections per heart, collected at 200 μm intervals) was performed. The differentiation of CDCs into myocytes and

endothelial cells was identified by immunostaining (6 sections per heart, collected at 400 µm intervals) with antibodies against GFP, α-sarcomeric actin and von Willebrand factor (vWf). Host cardiomyocyte cell cycle re-entry was evaluated by immunostaining (6 sections per heart, collected at 400 µm intervals) with antibodies against α-sarcomeric actin, Ki67 and BrdU. Recruitment of endogenous progenitors was assessed by immunostaining (6 sections per heart, collected at 400 µm intervals) against c-Kit. Vessel density in the infarct border zone was evaluated by immunostaining (6 sections per heart, collected at 400 µm intervals) with antibodies against vWf. In all sections used for immunohistochemistry, Alexa Fluor conjugated secondary antibodies (Molecular probes) were used and counterstaining with 4,6-diamidino-2-phenylindole (DAPI, Molecular Probes) was performed. Sections were imaged using a confocal laser scan microscope (Leica Microsystems) and images were processed by Leica LAS software suite. All antibodies used for immunohistochemistry are listed in supplemental table 3.

Assessment of systemic immunogenicity and development of memory immune response

In order to assess the systemic immunogenicity of CDC transplantation, levels of circulating inflammatory cytokines were measured in rat sera isolated from recipients of syngeneic, allogeneic, xenogeneic CDCs and controls. The levels of circulating IFN-g, IL-1b, IL-13, IL-4, IL-5, KC/GRO and TNF-α were quantified by electrochemiluminescence.

In order to assess development of humoral memory immune response, recipient rat sera were isolated at 1 week and 3 weeks post transplantation and levels of circulating alloreactive and xenoreactive anti-donor antibodies were quantified by flow cytometry. In brief, rCDCs and hCDCs were incubated with 50 µl of rat serum samples isolated from syngeneic, allogeneic and xenogeneic recipients or with naïve rat serum (isotype control) for 30 min on ice. After washing, cells were incubated with anti-rat IgM and anti-rat IgG antibodies for 30 min on ice. Cells were

analyzed in a benchtop flow cytometer (FACSCalibur; BD Biosciences, San Jose, Ca) and quantitative analysis was performed using CellQuest software (BD Biosciences).

In order to assess development of cellular memory immune response, spleens from allogeneic recipients were harvested at 3 weeks post transplantation. Lymphocytes were isolated and their reactivity against allogeneic donor cells was assessed by one-way mixed lymphocyte cocultures and was compared to that of naïve lymphocytes. The cell-free supernatant of the cocultures was collected and the levels of secreted IFN-g, IL-1b, IL-13, IL-4, IL-5, KC/GRO and TNF-α were measured by electrochemiluminescence. The levels of secreted IL-2 were measured using ELISA kits, according to the manufacturer's protocols (R&D Systems)

Electrochemiluminescence

Electrochemiluminescence was performed to assess levels of inflammatory cytokines in: a) serum samples obtained from rats injected with syngeneic, allogeneic, xenogeneic CDCs or vehicle, at 3 weeks post injection; b) cell culture supernatants obtained from co-cultures of lymphocytes with syngeneic, allogeneic and xenogeneic CDCs. Rat serum samples and cell culture supernatants were assayed for levels of IFN-g, IL-1b, IL-13, IL-4, IL-5, KC/GRO and TNF-α using a commercially available, ruthenium based electrochemoluminescence platform (Meso Scale Discovery, Gaithersburg, MD) following the manufacturer's recommendations. Samples were thawed and centrifuged with 15,000 rcf for 15 min right before use. All samples were run in duplicate using 25 µl of rat serum or supernatant per well. Results were considered valid when recovery (expected concentration divided by calculated concentration multiplied by 100) was 100±20%, percentage of coefficient of variation (CV = average of replicates divided by the standard deviation multiplied by 100) was <20%, intraassay CV was <10% and interassay CV was <20%. A spike-recovery protocol was initiated that allowed control for possible matrix

effects when comparing levels of cytokines between serum and supernatant. Results were considered valid if 85% of the samples of a run met these specifications.

Western Blotting

Western blot analysis was performed to compare the myocardial levels of VEGF, IGF-1 and HGF at various time points post MI among rats treated with syngeneic CDCs, allogeneic CDCs, xenogeneic CDCs and controls. Myocardial samples from the peri-infarct area were collected at 5 minutes, 1 day, 4 days, 7 days and 21 days post MI. Tissue samples were lysed in lysis buffer supplemented with proteinase inhibitors cocktail (Roche) and homogenized with a rotor-stator homogenizer. Homogenates were centrifuged at 12,000 rcf for 15 minutes at 4°C, supernatants were collected and protein content was quantified by Lowry assay (BioRad). The equivalent of 15 μg of total protein per lane was loaded onto 12% Precise Protein gels, and then transferred to PVDF membranes. Membranes were blocked with 5% non-fat milk and incubated overnight with primary antibodies against VEGF, IGF, HGF and GAPDH. Subsequently, the appropriate horseradish peroxidase-conjugated secondary antibodies were used, and then the blots were visualized by using SuperSignal West Femto maximum sensitivity substrate (Thermo Scientific) and exposed to Gel Doc XR System (Bio-Rad Lab. Inc.).Quantitative analysis was performed by ImageJ software, and expressions were normalized to GAPDH.

Supplemental tables

Experiment	**n**
Flow cytometric analysis of rCDCs (Fig 1)	9
Flow cytometric analysis of hCDCs (Fig 1)	9
MLR: responder cell proliferation syngeneic grp (Fig 2b)	6
MLR: responder cell proliferation allogeneic grp (Fig 2b)	6
MLR: responder cell proliferation xenogeneic grp (Fig 2b)	8
MLR: responder cell proliferation sensitized grp (Supp Fig3b)	8
MLR: cytokine levels in supernatant syngeneic grp (ECL+ELISA) (Fig 2c)	25
MLR: cytokine levels in supernatant allogeneic grp (ECL+ELISA) (Fig 2c)	26
MLR: cytokine levels in supernatant xenogeneic grp (ECL+ELISA) (Fig 2c)	21
MLR: cytokine levels in supernatant sensitized grp (ECL+ELISA) (Supp Fig 3c)	28
PCR syngeneic grp (Fig 3C, 3D)	12
PCR allogeneic grp (Fig 3C, 3D)	12
PCR xenogeneic grp (Fig 3C, 3D)	10
Masson’s Trichrome syngeneic grp (Fig 4A-C)	7
Masson’s Trichrome allogeneic grp (Fig 4A-C)	8

Masson’s Trichrome xenogeneic grp (Fig 4A-C)	5
Masson’s Trichrome control grp (Fig 4A-C)	5
Echocardiography syngeneic grp day 0(Fig 4D-F)	23
Echocardiography syngeneic grp 3 weeks(Fig 4D-F)	23
Echocardiography syngeneic grp 3 months(Fig 4D-F)	7
Echocardiography syngeneic grp 6 months(Fig 4D-F)	7
Echocardiography syngeneic grp FAC treatment effect (Fig 4F)	23
Echocardiography allogeneic grp day 0(Fig 4D-F)	21
Echocardiography allogeneic grp 3 weeks(Fig 4D-F)	21
Echocardiography allogeneic grp 3 months(Fig 4D-F)	7
Echocardiography allogeneic grp 6 months(Fig 4D-F)	7
Echocardiography allogeneic grp FAC treatment effect (Fig 4F)	21
Echocardiography control WKY grp day 0(Fig 4D-F)	11
Echocardiography control WKY 3 weeks(Fig 4D-F)	11
Echocardiography control WKY 3 months(Fig 4D-F)	6
Echocardiography control WKY 6 months(Fig 4D-F)	6
Echocardiography control WKY FAC treatment effect (Fig 4F)	11
Echocardiography control BN grp day 0 (Fig 4D-F)	11

Echocardiography control BN 3 weeks(Fig 4D-F)	11
Echocardiography control BN 3 months(Fig 4D-F)	6
Echocardiography control BN 6 months(Fig 4D-F)	6
Echocardiography control BN grp FAC treatment effect (Fig 4F)	11
Echocardiography xenogeneic grp day 0 (Fig 4D-G)	10
Echocardiography xenogeneic grp 3 weeks (Fig 4D-F)	10
Echocardiography xenogeneic grp FAC treatment effect (Fig 4F)	10
H&E syngeneic grp (Fig 5, Supp Fig 5)	13
H&E allogeneic grp (Fig 5, Supp Fig 5)	13
H&E control grp (Fig 5, Supp Fig 5)	13
H&E xenogeneic grp (Fig 5)	9
IHC syngeneic grp (Fig 6, Supp Fig 5)	11
IHC allogeneic grp (Fig 6, Supp Fig 5)	11
IHC control grp (Fig 6, Supp Fig 5)	11
IHC xenogeneic grp (Fig 6)	8
IHC syngeneic grp (Fig 7)	21
IHC allogeneic grp (Fig 7)	21
IHC control grp (Fig 7)	21

Western blot syngeneic grp (Fig 8)	20
Western blot allogeneic grp (Fig 8)	20
Western blot WKY control grp (Fig 8, Sup Fig 6)	15
Western blot BN control grp (Fig 8, Sup Fig 6)	15
Western blot WKY xenogeneic grp (Sup Fig 6)	20
Flow cytometry anti-donor antibodies syngeneic grp (Supp Fig 2)	12
Flow cytometry anti-donor antibodies allogeneic grp (Supp Fig 2)	12
Flow cytometry anti-donor antibodies xenogeneic grp (Supp Fig 2)	14
ECL serum cytokines syngeneic grp (Supp Fig 1)	21
ECL serum cytokines allogeneic grp (Supp Fig 1)	18
ECL serum cytokines xenogeneic grp (Supp Fig1)	20
ECL serum cytokines control grp (Supp Fig 1)	5

Supplemental Table 1. Sample sizes

Name	#1	#2	#3	#4	#5	#6	#7
Age	56	54	52	45	69	62	49
Male/female	M	M	M	M	M	M	M
Weight (kg)	85.7	63.2	71.4	81.2	87.7	68	107
Body mass index	29.6	22.5	26.2	26.4	32.2	25	34.9
Smoker	N	N	Y	N	N	N	Y
Diabetes	N	N	N	N	N	N	Y
Hyperlipidemia	Y	Y	Y	Y	Y	N	Y
Renal dysfunction	N	N	N	N	N	Y	Y
Hypertension	Y	Y	N	Y	Y	Y	Y
Chronic lung disease	N	N	N	N	N	N	N
Peripheral vascular disease	N	N	N	N	Y	N	Y
Cerebrovascular disease	N	N	N	N	N	N	N
Myocardial infarction	Y	Y	Y	Y	Y	N	Y
Coronary artery disease	Y	Y	Y	Y	Y	N	Y
Angina	N	N	N	N	N	N	Y
Arrhythmia	N	N	N	N	N	N	Y
Congestive heart failure	N	N	N	N	N	Y	Y
Classification NYHA (I/II/III/IV)	N	N	N	N	N	IV	IV
Cardiac surgical procedure (CABG/valve/DOR)	N	N	N	N	N	N	N

Other surgical procedures	Y (Colon Resection)	N	N	N	Y (S/P Gastric Resection)	N	N
Other comorbidities	Diverticulitis	N	N	N	Peptic Ulcer Disease	Amyoloidosis, Peptic Ulcer Disease, Cholelithiasis, Nephrolithiasis	Gout
Medications							
Aspirin	Y	Y	Y	Y	Y	N	Y
Clopidogrel	Y	Y	Y	Y	Y	N	N
Statins	Y	Y	Y	Y	Y	N	Y
Amiodarone	N	N	N	N	N	N	N
Angiotensin-converting enzyme inhibitors/ angiotensin receptor blockers	Y	Y	Y	Y	N	N	N
Beta Blocker	Y	Y	Y	Y	Y	Y	Y
Ca++ Blocker	N	N	N	N	N	N	N
Nitrate	N	N	N	N	N	N	N

Supplemental Table 2. Human (xenogeneic) cell donor characteristics

Antigen	Antibody	Procedure
HLA-A,B,C	PE Mouse Anti-Human HLA-ABC (BD Pharmingen)	FC
HLA-A,B,C	APC Mouse Anti-Human HLA-ABC (BD Pharmingen)	FC
HLA-DR,DP,DQ	FITC Mouse Anti-Human HLA-DR,DP,DQ (BD Pharmingen)	FC
CD86	APC Mouse Anti-Human CD86 (BD Pharmingen)	FC
CD80	FITC Mouse Anti-Human CD80 (BD Pharmingen)	FC
RT1A	PE Mouse Anti-Rat RT1A (BD Pharmingen)	FC
RT1D	FITC Mouse Anti-Rat RT1D (BD Pharmingen)	FC
CD80	PE Mouse Anti-Rat CD80 (BD Pharmingen)	FC
CD80	FITC Mouse Anti-Rat CD80 (AbD Serotec)	FC
CD86	FITC Mouse Anti-Rat CD86 (BD Pharmingen)	FC
CD90	PE Mouse Anti-Human CD90 (BD Pharmingen)	FC
CD31	Alexa Fluor 647 Mouse Anti-Human CD31 (BD Pharmingen)	FC
CD45	APC Mouse anti-Human CD45 (BD Pharmingen)	FC
CD105	PE Mouse anti-Human CD105 (R&D systems)	FC
DDR2	Mouse anti-Human CD105 (R&D systems)	FC
αSMA	PE Mouse anti-Human α-SMA (R&D systems)	FC

CD140b	Mouse anti-Human CD140b (BD Pharmingen)	FC
CD90	FITC Mouse anti-Rat CD90 (BD Pharmingen)	FC
CD45	FITC Mouse anti-rat CD45 (BD Pharmingen)	FC
CD31	PE Mouse anti-Rat CD31 (BD Pharmingen)	FC
CD105	Mouse anti-Rat CD105 (Novus Biologicals/Abcam)	FC
DDR2	Rabbit anti-Rat DDR2 (Santa Cruz/Abcam)	FC/ICC
αSMA	Rabbit anti-Rat αSMA	FC
CD140b	Rabbit anti-Rat CD140b	FC
c-Kit	rabbit anti-human/rat/ (Santa Cruz)	FC, IHC
CD3	Rabbit anti-rat CD3 (Abcam)	IHC
CD45RA	Mouse anti-rat CD45RA (Abcam)	IHC
CD45RA	Mouse anti-rat CD45RA (AbD Serotec)	IHC
CD8	Rabbit anti-rat CD8 (Abcam)	IHC
CD4	Mouse anti-rat CD4 (Abcam)	IHC
CD11c	Mouse anti-rat CD11c (Abcam)	IHC
CD68	Rabbit Anti-rat CD68 (Abbiotec)	IHC
CD68	Mouse anti-rat CD68 (AbD Serotec)	IHC
CD8	Mouse anti-rat CD8 (AbD Serotec)	IHC
CD4	Mouse anti-rat CD4 (BD Pharmingen)	IHC

CD11c	Mouse anti-rat CD11c (BD Pharmingen)	IHC
GFP	Goat anti-GFP (Abcam)	IHC
α-smooth muscle actin	Rabbit anti-rat α-smooth muscle actin (Abcam)	IHC
α-sarcomeric actinin	Rabbit anti-rat α-sarcomeric actinin (Abcam)	IHC
Von Willebrand Factor	Rabbit anti-rat vWF (Abcam)	IHC
α-sarcomeric actinin	Mouse anti-rat α-sarcomeric actinin (Sigma)	IHC
α-smooth-muscle actin	Mouse anti-rat α-smooth-muscle actin (Abcam)	IHC
Ki67	Rabbit anti-rat Ki67 (Abcam)	IHC
Ki67	Rabbit anti-rat Ki67 (Thermo)	IHC
BrdU	Mouse anti-BrdU (Roche)	IHC
Goat IgG	Alexa Fluor 488 donkey anti-goat IgG (Molecular Probes)	IHC
Mouse IgG	Alexa Fluor 546 donkey anti-mouse IgG (Molecular Probes)	IHC
Rabbit IgG	Alexa Fluor 647 donkey anti-rabbit IgG (Molecular Probes)	IHC
VEGF	Mouse anti-rat VEGF (Abcam)	WB
IGF1	Mouse monoclonal to IGF1 (Abcam)	WB

HGF	Rabbit anti-rat HGF (Abcam)	WB
VEGF	Mouse anti-rat/human VEGF (Abcam)	WB
IGF1	Goat anti-rat/human IGF1 (Abcam)	WB
HGF	Rabbit anti-rat/human HGF	WB
Mouse IgG	Goat anti-mouse IgG, HRP-conjugated (Cell Signaling)	WB
Rabbit IgG	Goat anti-rabbit IgG, HRP-conjugated (Cell Signaling)	WB
Goat IgG	Donkey anti-goat IgG, HRP-conjugated (Abcam)	WB
Rat IgM	FITC Mouse Anti-Rat IgM (BD Pharmingen)	FC
Rat IgG1/2a	FITC Mouse Anti-Rat IgG1/2a (BD Pharmingen)	FC

Supplemental Table 3. List of antibodies

Groups	Peri-operative mortality	Longer-term mortality
Syngeneic	4/47 (8.5%)	3/43 (6.9%)
Allogeneic	4/46 (8.7%)	2/42 (4.8%)
Control WKY	2/25 (8.0%)	3/23 (13.1%)
Control BN	3/25 (12.0%)	2/22 (9.1%)
Xenogeneic	4/48 (8.3%)	4/44 (9.1%)

Supplemental Table 4. Peri-operative and longer-term mortality (post-operative period until protocol completion). Ns denote animals that died; (ns) denote mortality rates

	Infarct area			Peri-infarct area			Remote myocardium		
	Patchy infiltration	***Diffuse infiltration***	***Myocyte damage***	***Patchy infiltration***	***Diffuse infiltration***	***Myocyte damage***	***Patchy infiltration***	***Diffuse infiltration***	***Myocyte damage***
Syngeneic (n=4)	**4/48* (2/4)**	**0/48 (0/4)**	**0/48 (0/4)**	**4/48* (2/4)**	**0/48 (0/4)**	**0/48 (0/4)**	**0/48 (0/4)**	**0/48 (0/4)**	**0/48 (0/4)**
Allogeneic (n=4)	**4/48* (1/4)**	**0/48 (0/4)**	**0/48 (0/4)**	**4/48* (1/4)**	**0/48 (0/4)**	**0/48 (0/4)**	**0/48 (0/4)**	**0/48 (0/4)**	**0/48 (0/4)**
Control (n=4)	**3/48* (1/4)**	**0/48 (0/4)**	**0/48 (0/4)**	**3/48* (1/4)**	**0/48 (0/4)**	**0/48 (0/4)**	**0/48 (0/4)**	**0/48 (0/4)**	**0/48 (0/4)**
Xenogeneic (n=4)	**28/48 (4/4)**	**0/48 (0/4)**	**0/48 (0/4)**	**30/48 (4/4)**	**0/48 (0/4)**	**0/48 (0/4)**	**0/48 (0/4)**	**0/48 (0/4)**	**0/48 (0/4)**

Supplemental Table 5. Homemade grading system for rejection at 1 week post MI and cell transplantation

	Infarct area			Peri-infarct area			Remote myocardium		
	Patchy infiltration	***Diffuse infiltration***	***Myocyte damage***	***Patchy infiltration***	***Diffuse infiltration***	***Myocyte damage***	***Patchy infiltration***	***Diffuse infiltration***	***Myocyte damage***
Syngeneic (n=5)	**2/60* (1/5)**	**0/60 (0/5)**	**0/60 (0/5)**	**1/60* (1/5)**	**0/60 (0/5)**	**0/60 (0/5)**	**0/60 (0/5)**	**0/60 (0/5)**	**0/60 (0/5)**
Allogeneic (n=5)	**1/60* (1/5)**	**0/60 (0/5)**	**0/60 (0/5)**	**0/60* (1/5)**	**0/60 (0/5)**	**0/60 (0/5)**	**0/60 (0/5)**	**0/60 (0/5)**	**0/60 (0/5)**
Control (n=5)	**1/60* (1/5)**	**0/60 (0/5)**	**0/60 (0/5)**	**1/60* (1/5)**	**0/60 (0/5)**	**0/60 (0/5)**	**0/60 (0/5)**	**0/60 (0/5)**	**0/60 (0/5)**
Xenogeneic (n=5)	**45/60 (5/5)**	**0/60 (0/5)**	**0/60 (0/5)**	**39/60 (5/5)**	**0/60 (0/5)**	**0/60 (0/5)**	**0/60 (0/5)**	**0/60 (0/5)**	**0/60 (0/5)**

Supplemental Table 6. Homemade grading system for rejection at 3 weeks post MI and cell transplantation

	Infarct area			Peri-infarct area			Remote myocardium		
	Patchy infiltration	***Diffuse infiltration***	***Myocyte damage***	***Patchy infiltration***	***Diffuse infiltration***	***Myocyte damage***	***Patchy infiltration***	***Diffuse infiltration***	***Myocyte damage***
Syngeneic (n=4)	**1/48* (1/4)**	**0/48 (0/4)**	**0/48 (0/4)**	**2/48* (2/4)**	**0/48 (0/4)**	**0/48 (0/4)**	**0/48 (0/4)**	**0/48 (0/4)**	**0/48 (0/4)**
Allogeneic (n=4)	**1/48* (1/4)**	**0/48 (0/4)**	**0/48 (0/4)**	**2/48* (1/4)**	**0/48 (0/4)**	**0/48 (0/4)**	**0/48 (0/4)**	**0/48 (0/4)**	**0/48 (0/4)**
Control (n=4)	**2/48* (2/4)**	**0/48 (0/4)**	**0/48 (0/4)**	**2/48* (2/4)**	**0/48 (0/4)**	**0/48 (0/4)**	**0/48 (0/4)**	**0/48 (0/4)**	**0/48 (0/4)**

Supplemental Table 7. Homemade grading system for rejection at 6 months post MI and cell transplantation

Supplemental Figures

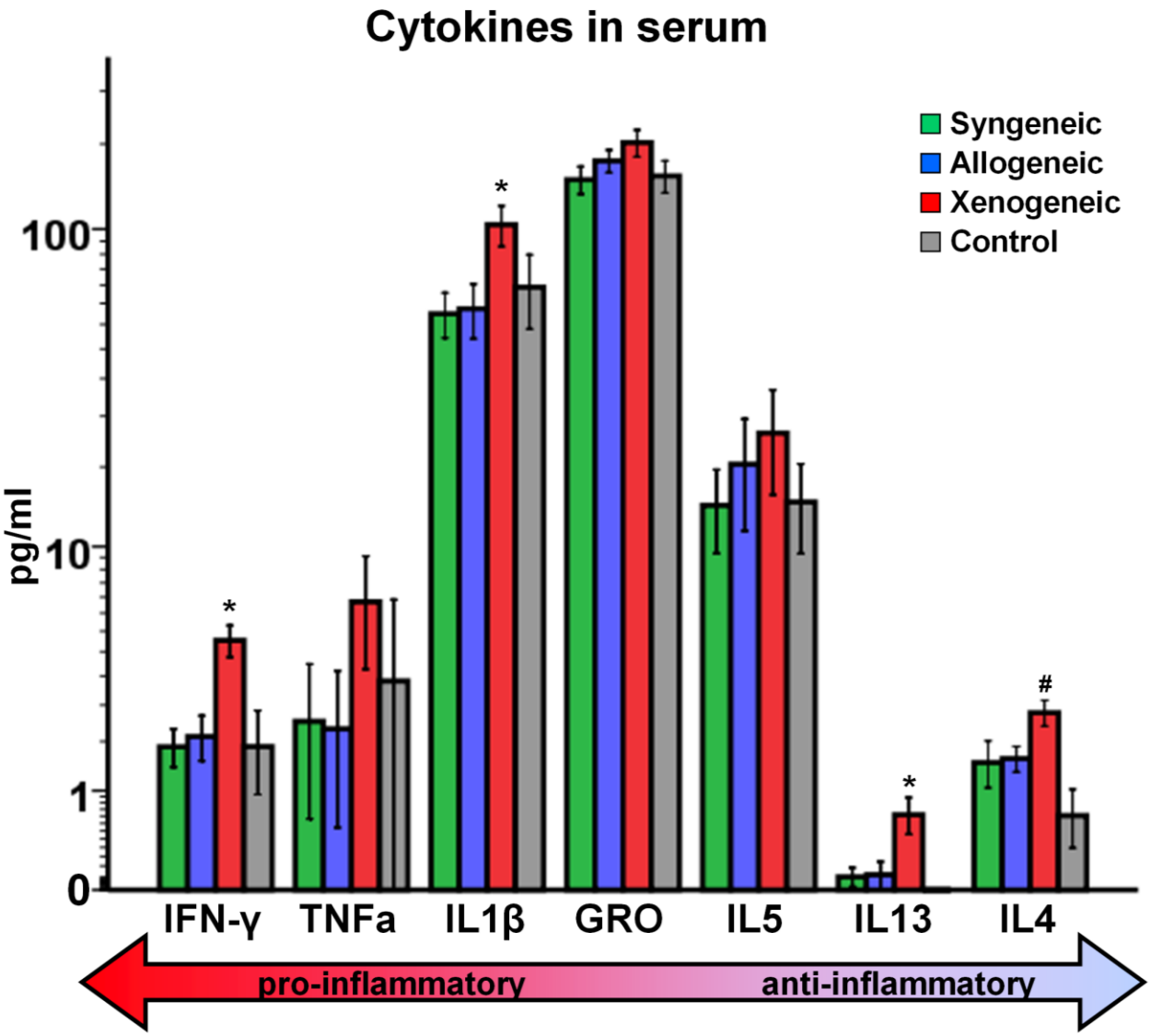

Supplemental Figure 1. Circulating levels of inflammatory cytokines measured with electrochemiluminescence in rat serum samples obtained 3 weeks post-treatment (n=5-21/group). (* $p<0.05$ compared to syngeneic, allogeneic groups; # $p<0.05$ compared to syngeneic, control groups)

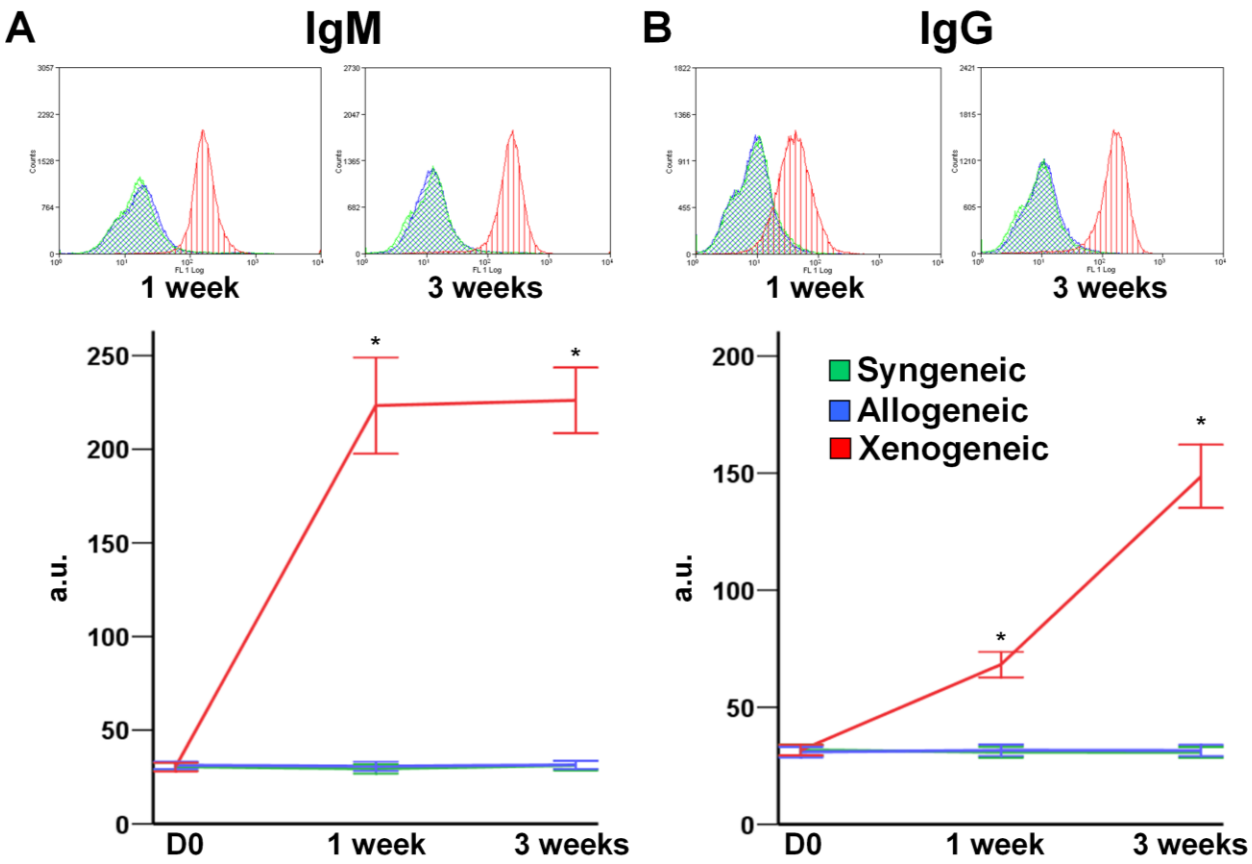

Supplemental Figure 2. Assessment of humoral memory response. Levels of circulating antidonor IgM (A) and IgG (B) antibodies were measured with flow cytometry at 1 week and 3 weeks post treatment (n=4/group at each timepoint). Allogeneic CDC transplantation (contrary to xenogeneic) did not generate detectable levels of circulating anti-donor antibodies. (* $p<0.05$ compared to syngeneic, allogeneic groups)

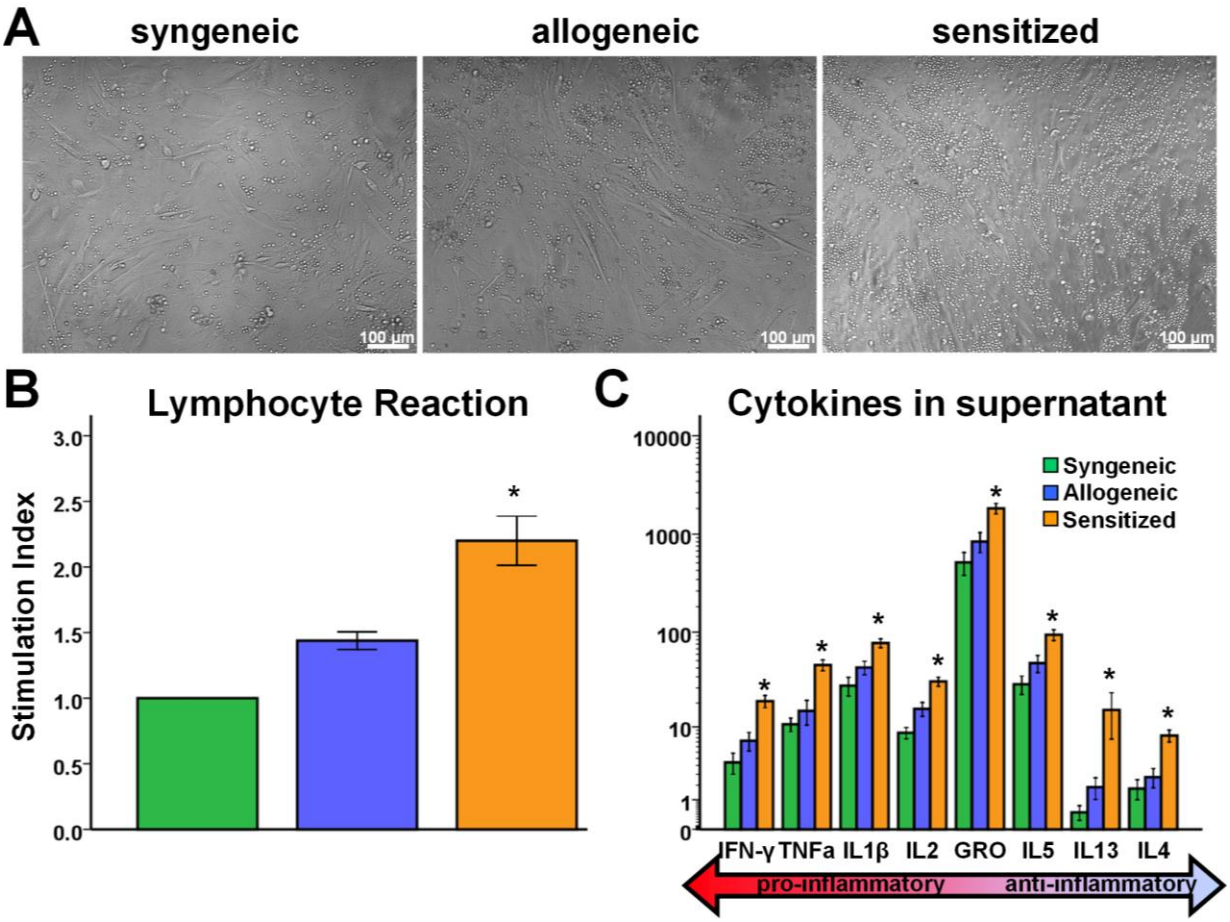

Supplemental Figure 3. Assessment of cellular memory response. (A) Representative images of syngeneic, naïve allogeneic and sensitized allogeneic cocultures. Significant lymphocyte proliferation can be observed in the sensitized allogeneic setting. Quantitative analyses of (B) responder cell proliferation (n= 6-8/group) and (C) inflammatory cytokine secretion (n=21-28/group). (* $p<0.05$ compared to syngeneic, allogeneic groups)

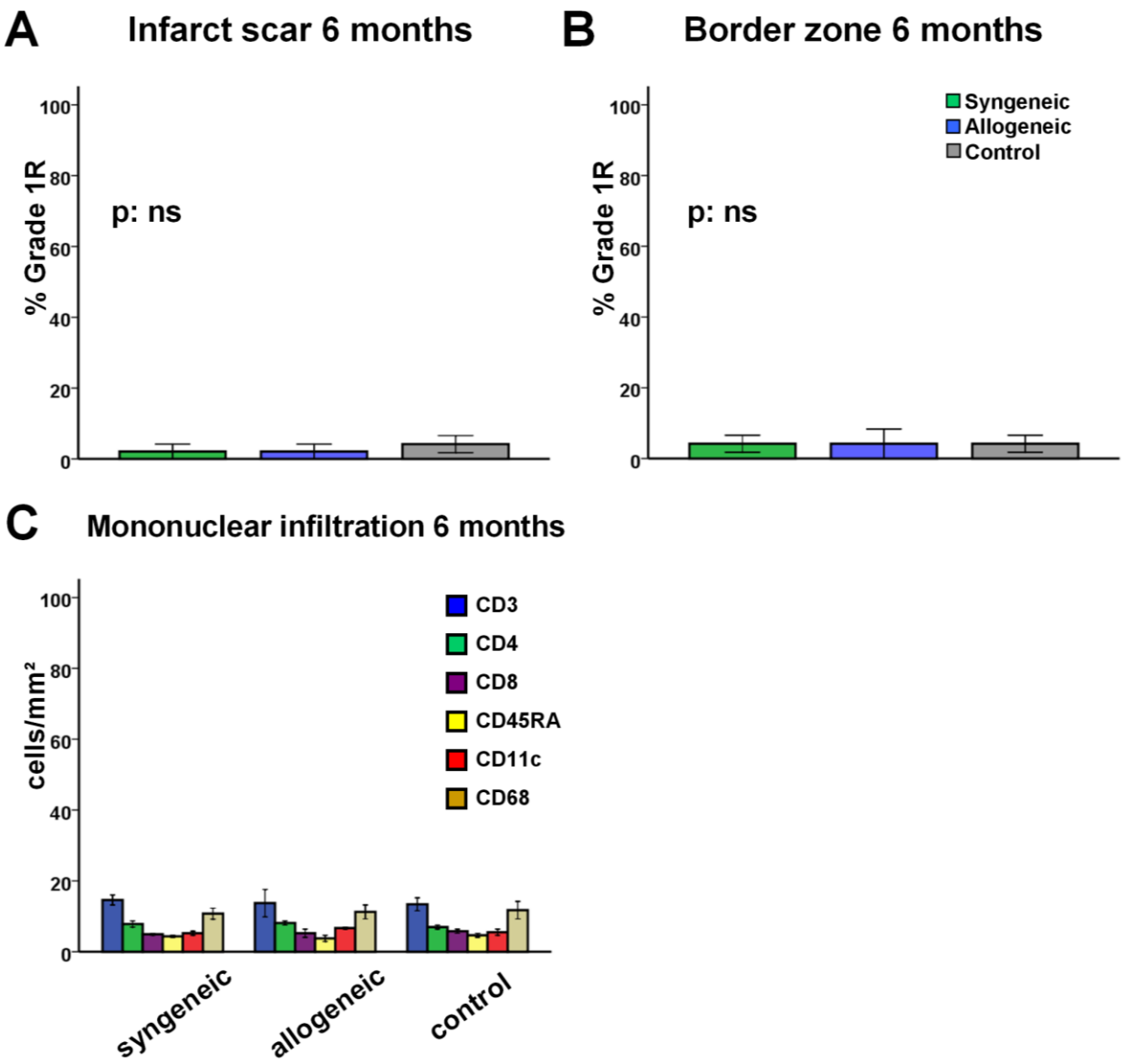

Supplemental Figure 4. Evaluation of immune reaction by H&E staining (A,B) (n=4/group) and immunohistochemistry (C) at 6 months post treatment (n=3/group). The mild immune reaction observed at 3 weeks had completely resolved by 6 months.

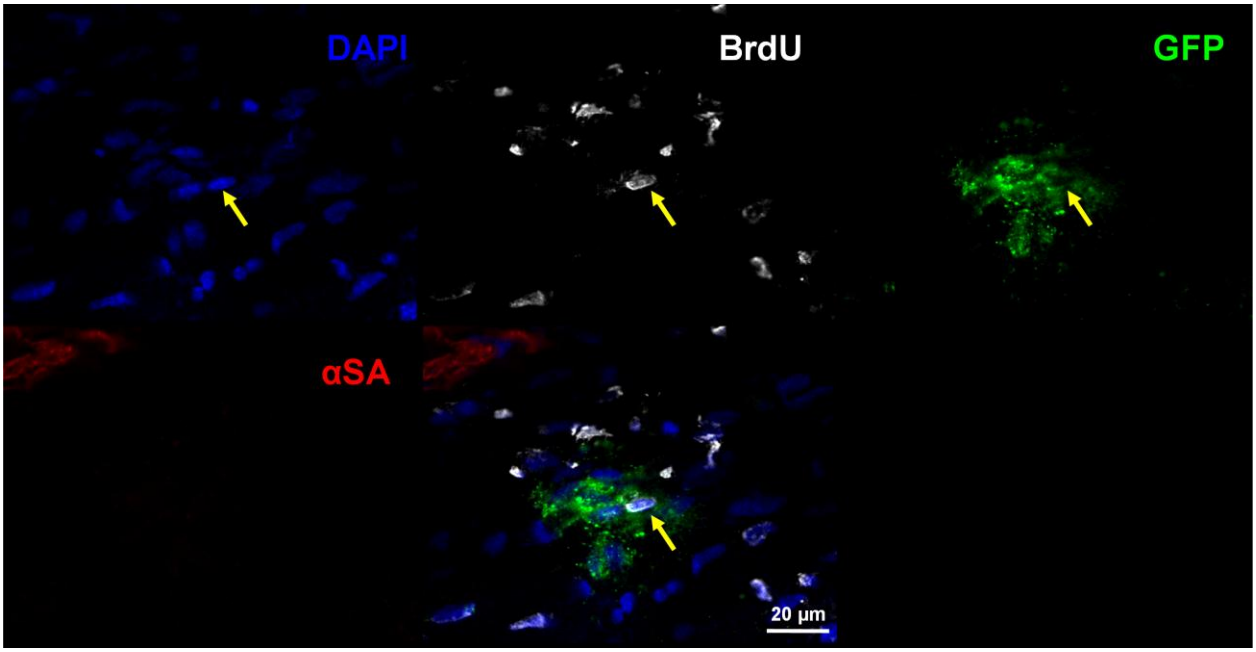

Supplemental Figure 5. A cluster of GFP+ CDCs in the peri-infarct area at 3 weeks post treatment. One CDC (arrow) is BrdU+ indicating *in vivo* proliferation.

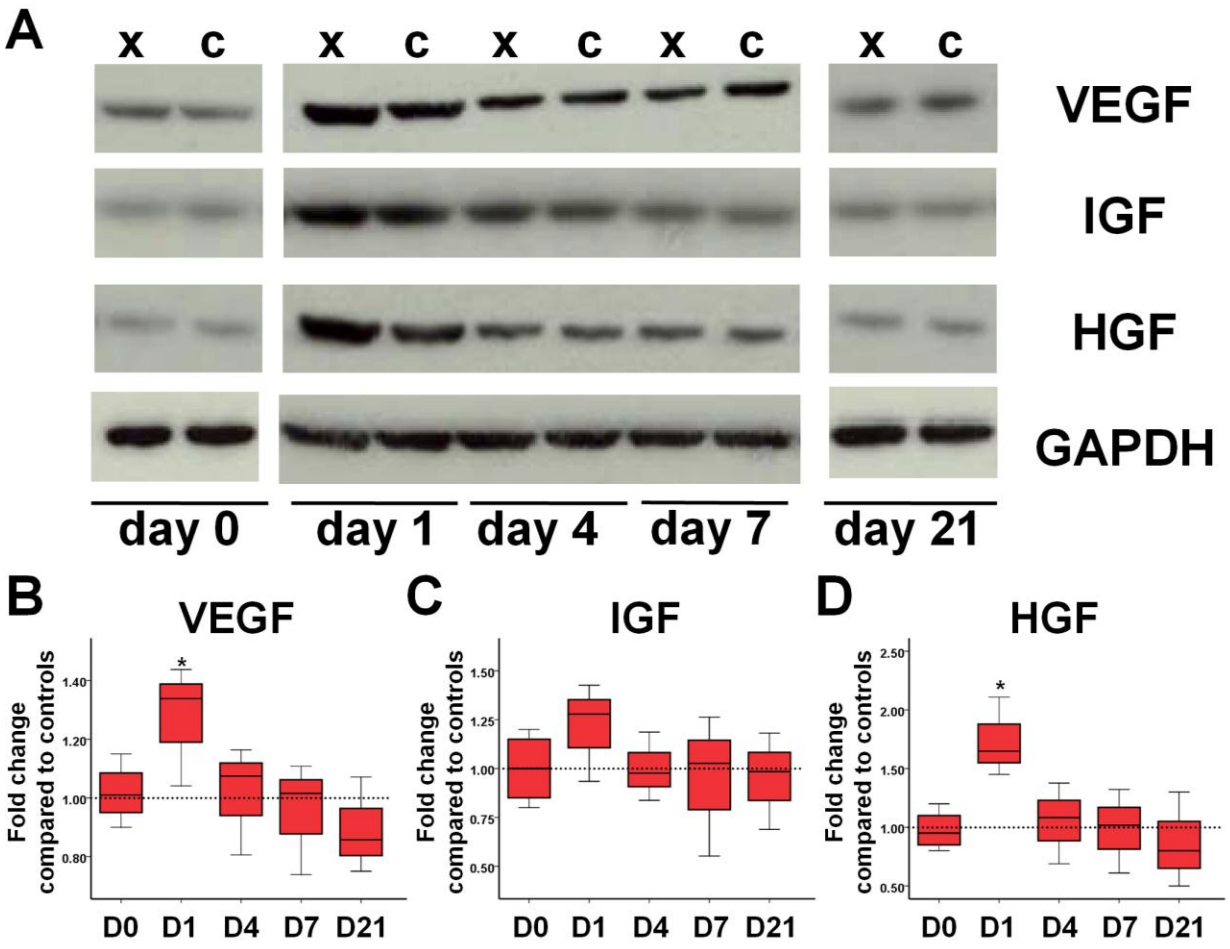

Supplemental Figure 6. Detection of beneficial paracrine factors by Western blotting in the xenogeneic group. (A) Representative blots demonstrating increased secretion of VEGF, IGF1 and HGF only at day1 post xenogeneic cell transplantation. No difference is observed at later time points. (B-D) Quantitative analysis of myocardial levels of VEGF (B), IGF-1 (C) and HGF (D) post-MI in the xenogeneic group (normalized to the control group; n=3/group at each timepoint). Only the levels at Day 1 are increased, consistent with the rapid clearance of xenogeneic transplanted CDCs (Fig. 3). (* $p<0.05$ compared to control group; x: xenogeneic; c: control)